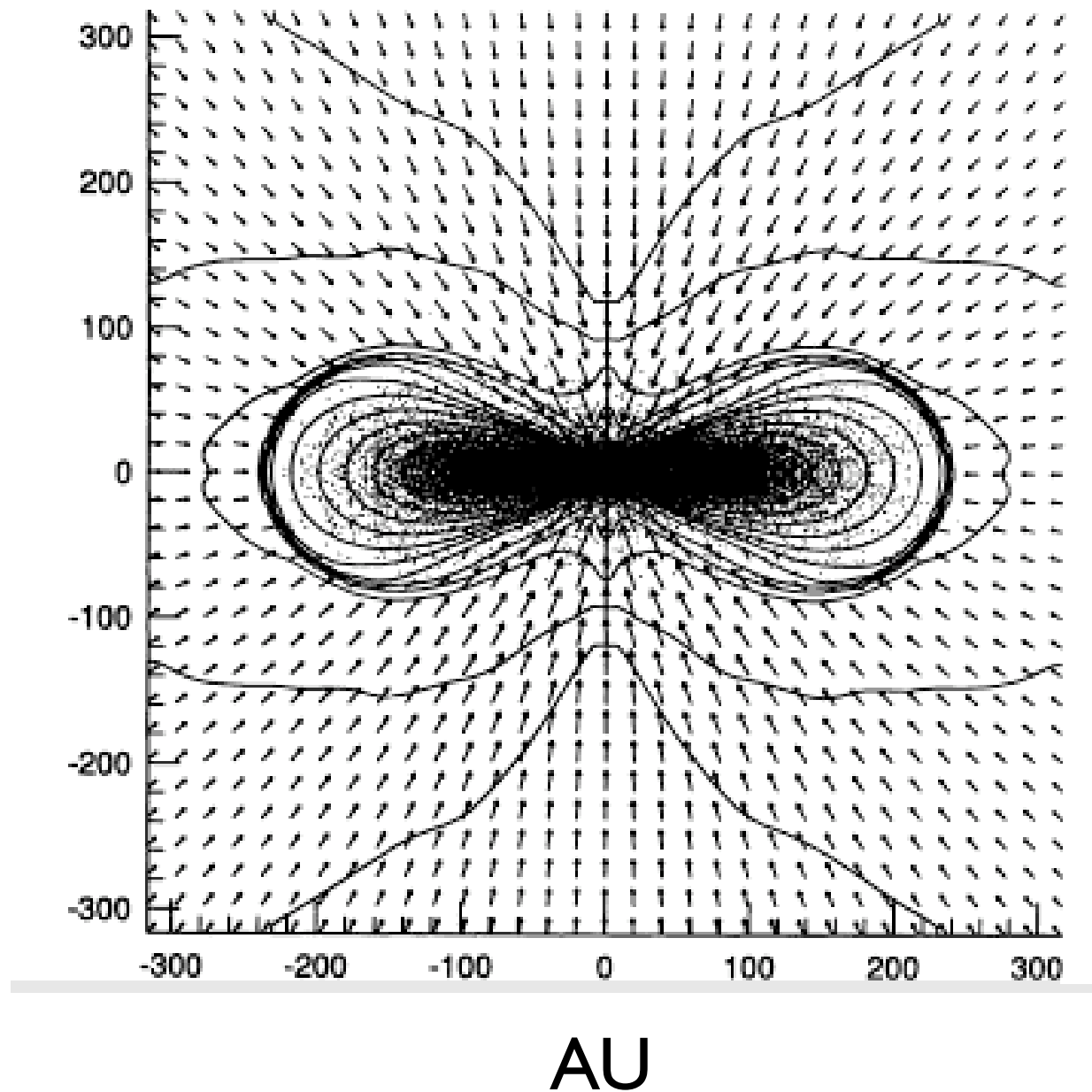


Background and History on Exoplanetary Science

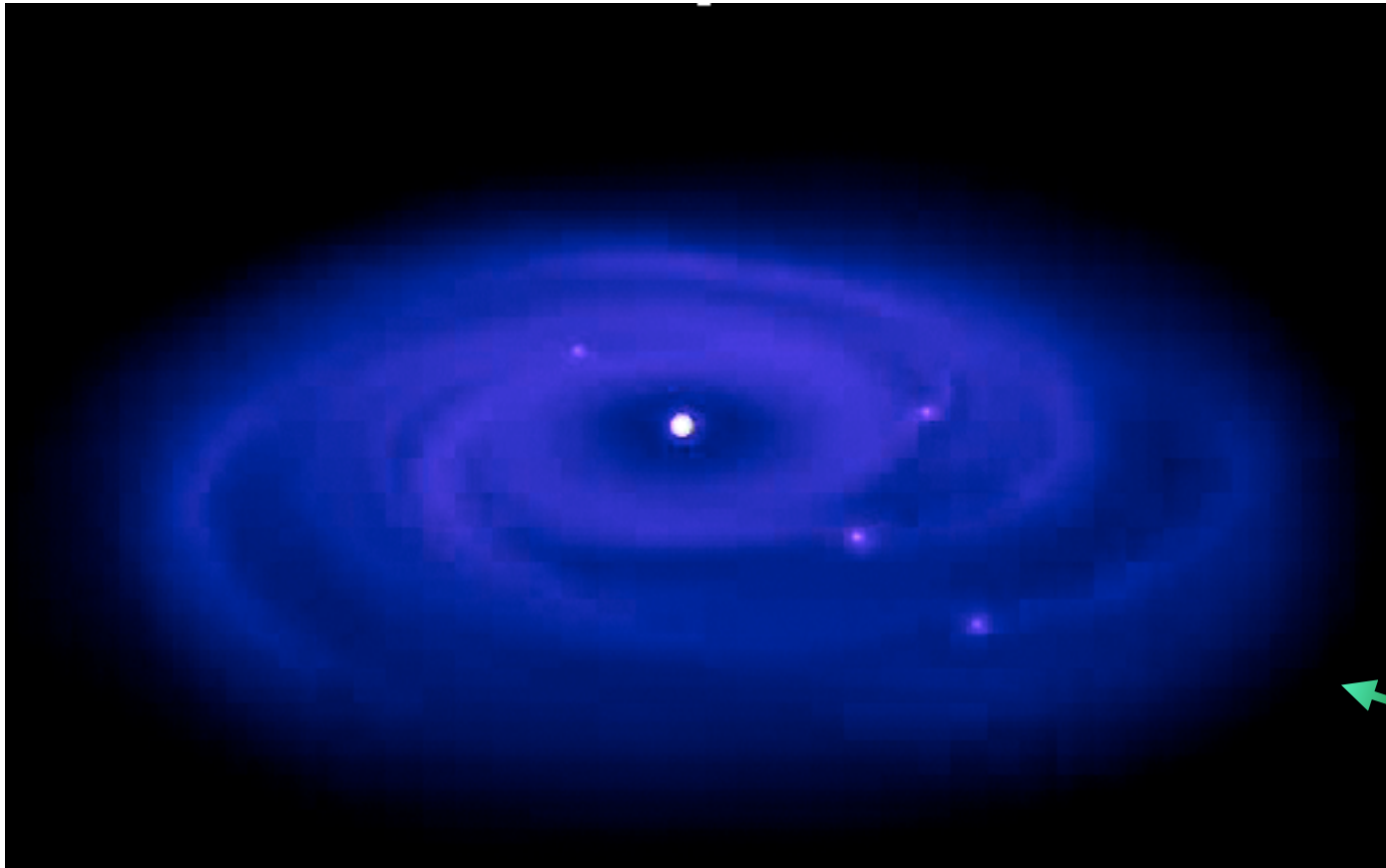
Greg Laughlin, UCSC



Simulation showing infall onto a massive protostellar disk



The Gravitational Instability Paradigm

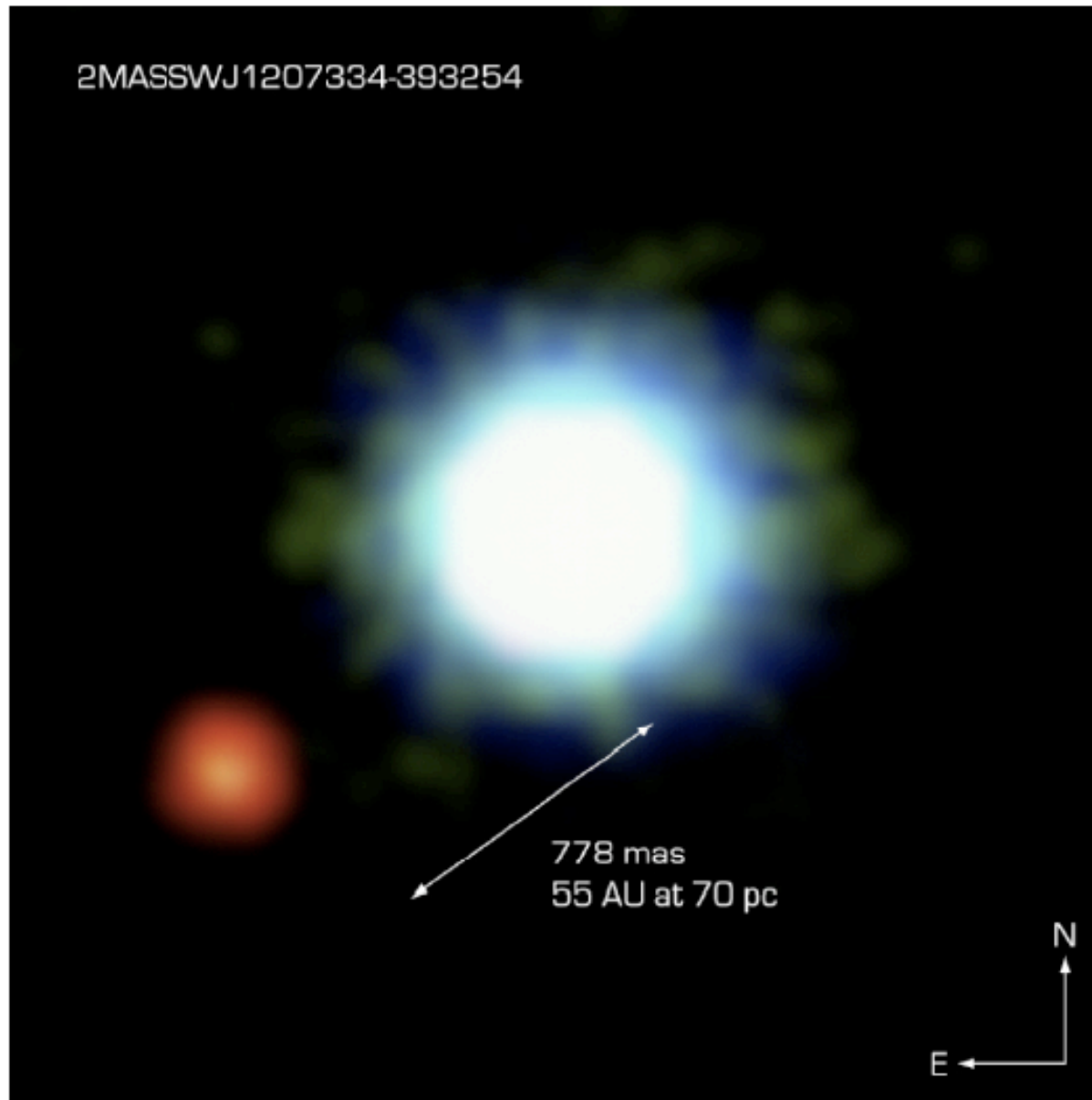


Kuiper 1951
Cameron 1978
DeCampli & Cameron 1979
Boss 1998
Boss 2000
Mayer et al. 2002
Pickett et al. 2003
Rice et al 2003a
Rice et al 2003b
Boss 2003
Cai et al 2004
Boss 2004
Mayer et al 2004
Mejia et al 2005
Boss 2006, 2007

Two basic requirements for gravitational disk instability to work:

1. $Q = \frac{c_s \kappa}{\pi G \sigma} \sim 1$ somewhere in the disk
2. The cooling time for fragments must be less than half an orbital period (Gammie (2001)).

2MASSWJ1207334-393254

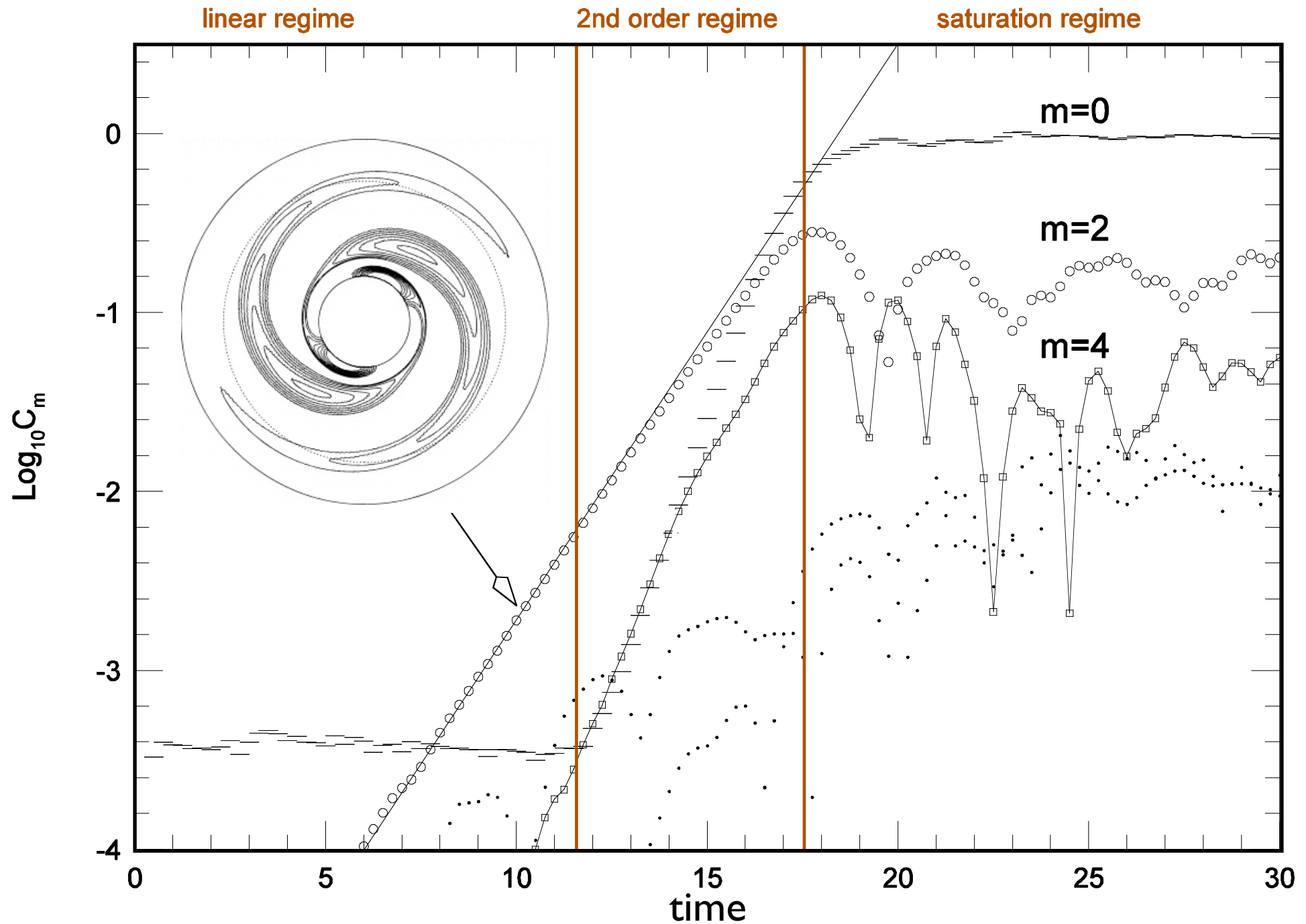


The Brown Dwarf 2M1207 and its Planetary Companion
(VLT/NACO)

ESO PR Photo 14a/05 (30 April 2005)



Objects like 2M1207b almost certainly formed through a process that involves some form of gravitational instability.



Another unresolved issue for G.I. is the feasibility of having a highly gravitationally unstable axisymmetric disk.

Name	PSR B1620-26 b
Discovered in	1994
Mass	$2.5 (\pm 1) M_J$
Semi major axis	$23 AU$
Orbital period	$36525 days$
Inclination	$55 deg.$



If GI constitutes a frequent mechanism for planet formation, then one expects to frequently find *Jovian-mass* planets in low-metallicity environments -- e.g. orbiting halo stars, solar neighborhood Pop II stars, globular clusters.

These planets are currently accessible to microlensing surveys, wide-field transit surveys and also to targeted RV surveys of metal-poor stars in the solar neighborhood.

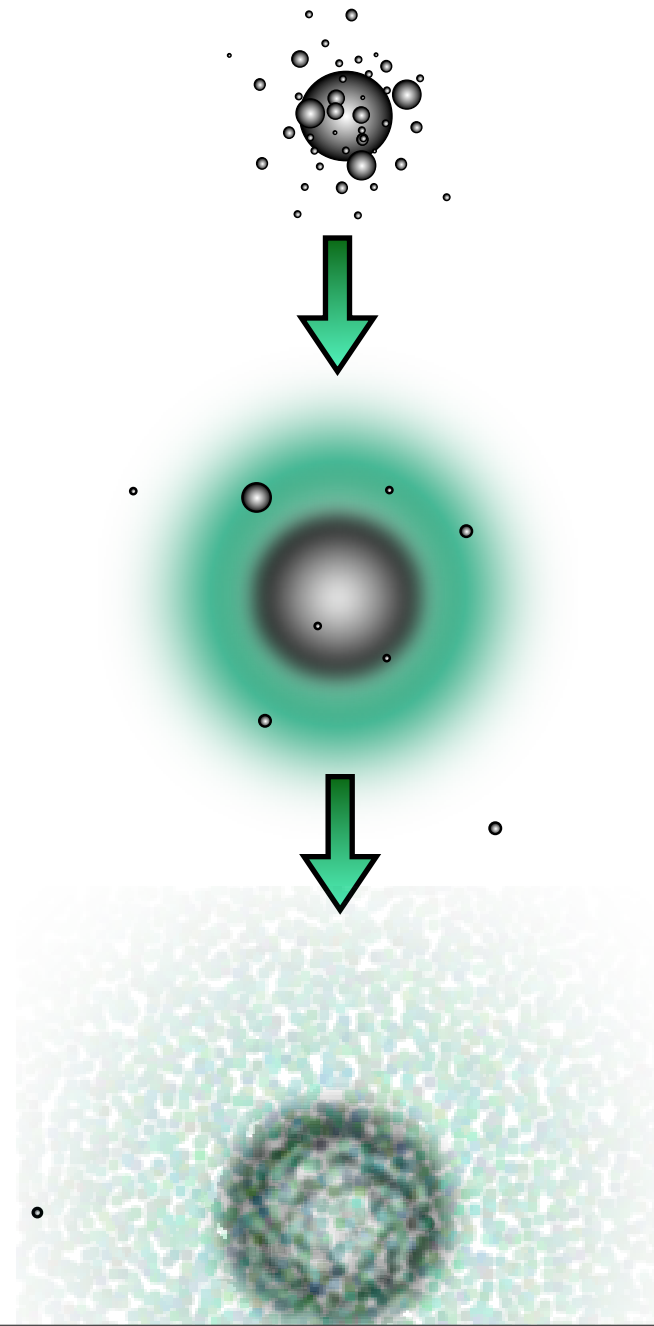
The Core Accretion Paradigm

Perri & Cameron 1974, Mizuno et al 1978, Mizuno 1980, Bodenheimer & Pollack 1986, Pollack et al 1996

During **Phase 1**, the growing planet consists mostly of solid material. The planet experiences runaway accretion until the feeding zone is depleted. Solid accretion occurs much faster than gas accretion during this phase.

During **Phase 2**, both solid and gas accretion rates are small and are nearly independent of time. This phase dictates the overall evolutionary time-scale.

During **Phase 3**, runaway gas accretion occurs. Runaway gas accretion starts when the solid and gas masses are roughly equal.



The Core Accretion Paradigm

(Pollack et al 1996)

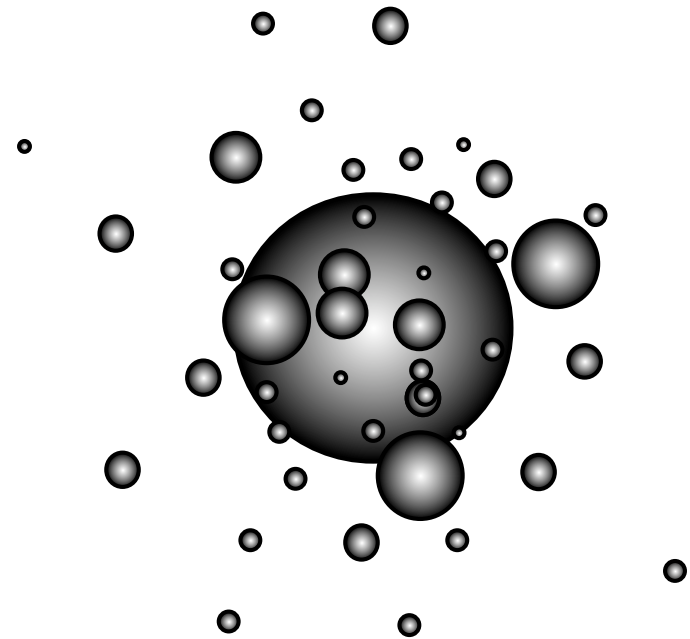
During **Phase I**, the mass increase of the planet depends on the planetary radius, and the ratio of the gravitational to geometric cross section:

$$\frac{dM_p}{dt} = \pi R_c^2 \sigma \Omega F_g$$

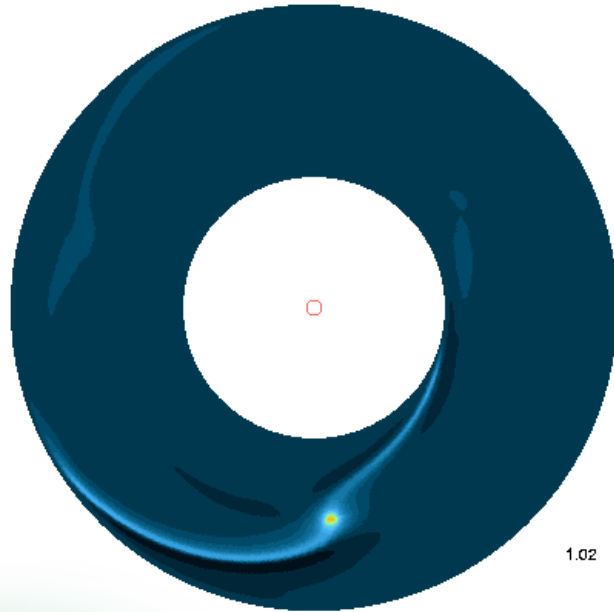
Because the escape velocity from the planetary surface is much faster than the relative velocity of planetesimals, this phase is characterized by a runaway growth of the solid core which ends when the core depletes its feeding zone, defined by:

$$a_f = \left(\sqrt{12 + e_h^2} \right) R_H$$

Hill Radius $\rightarrow R_H = a \left(\frac{M_P}{3M_\odot} \right)^{1/3}$



As runaway solid accretion proceeds through several Earth masses, the gas envelope becomes increasingly significant. Modeling of this stage requires computation of the hydrodynamic structure and effect of the gas envelope.



1. Stellar Evolution code for the quasi-equilibrium envelope:

$$\frac{dP}{dR} = -g\rho$$

$$\frac{dM}{dR} = 4\pi R^2 \rho$$

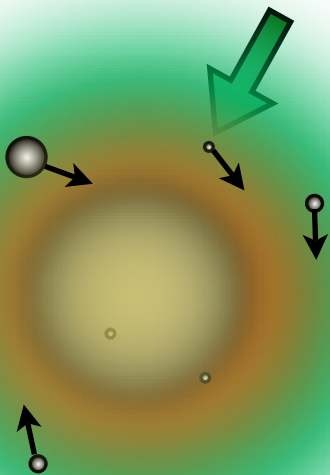
$$\frac{dT}{dR} = \frac{-3\kappa\rho}{16\sigma T^3} \frac{L}{4\pi R^2}$$

$$L_{core} = \frac{GM_{core}\dot{M}_{core}}{R_{core}}$$

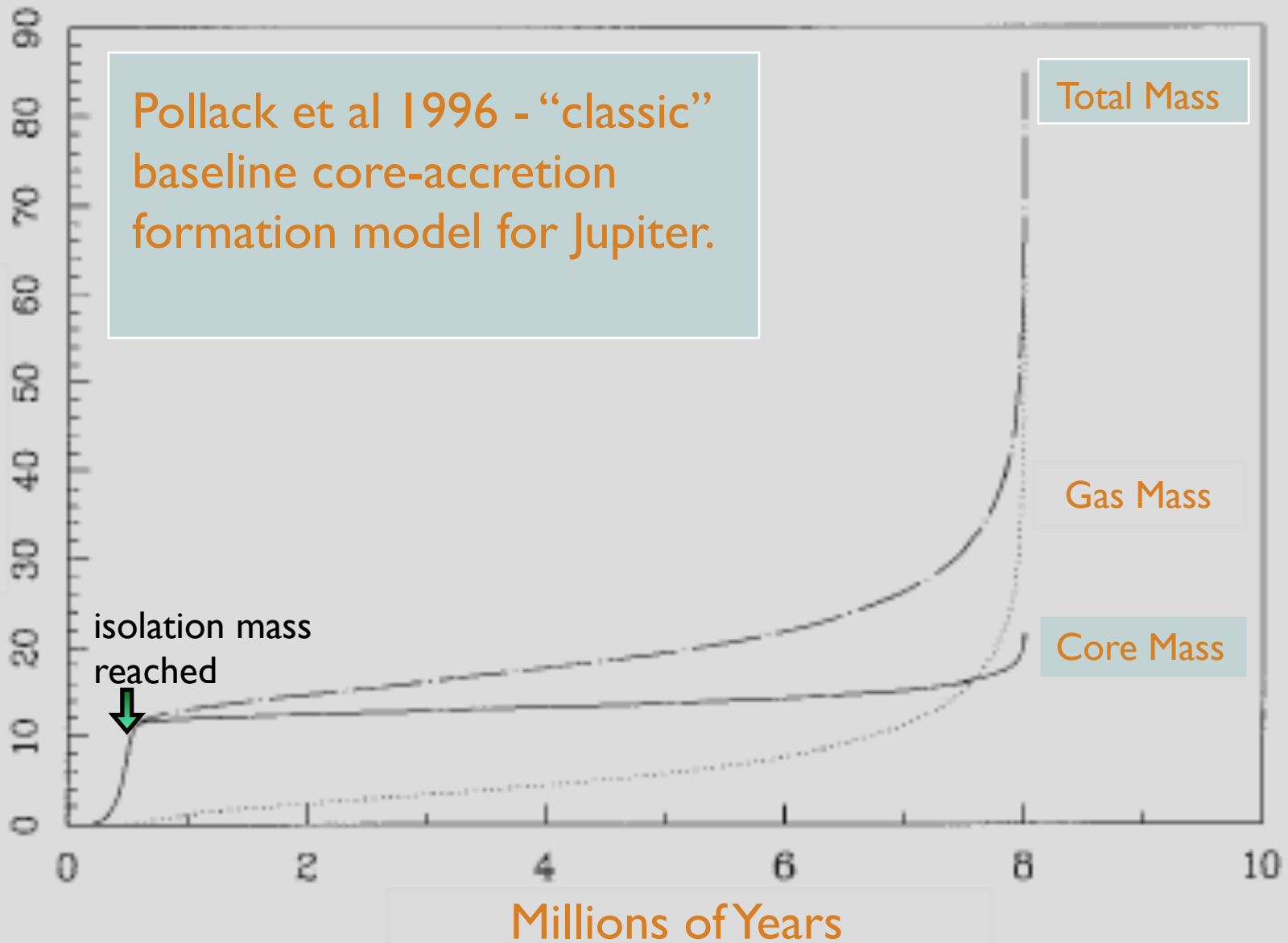
2. Planetesimal dissolution routine:

$$v_{encounter} = \left(\sqrt{\frac{5e^2}{8} + i^2} \right) v_{kepler}$$

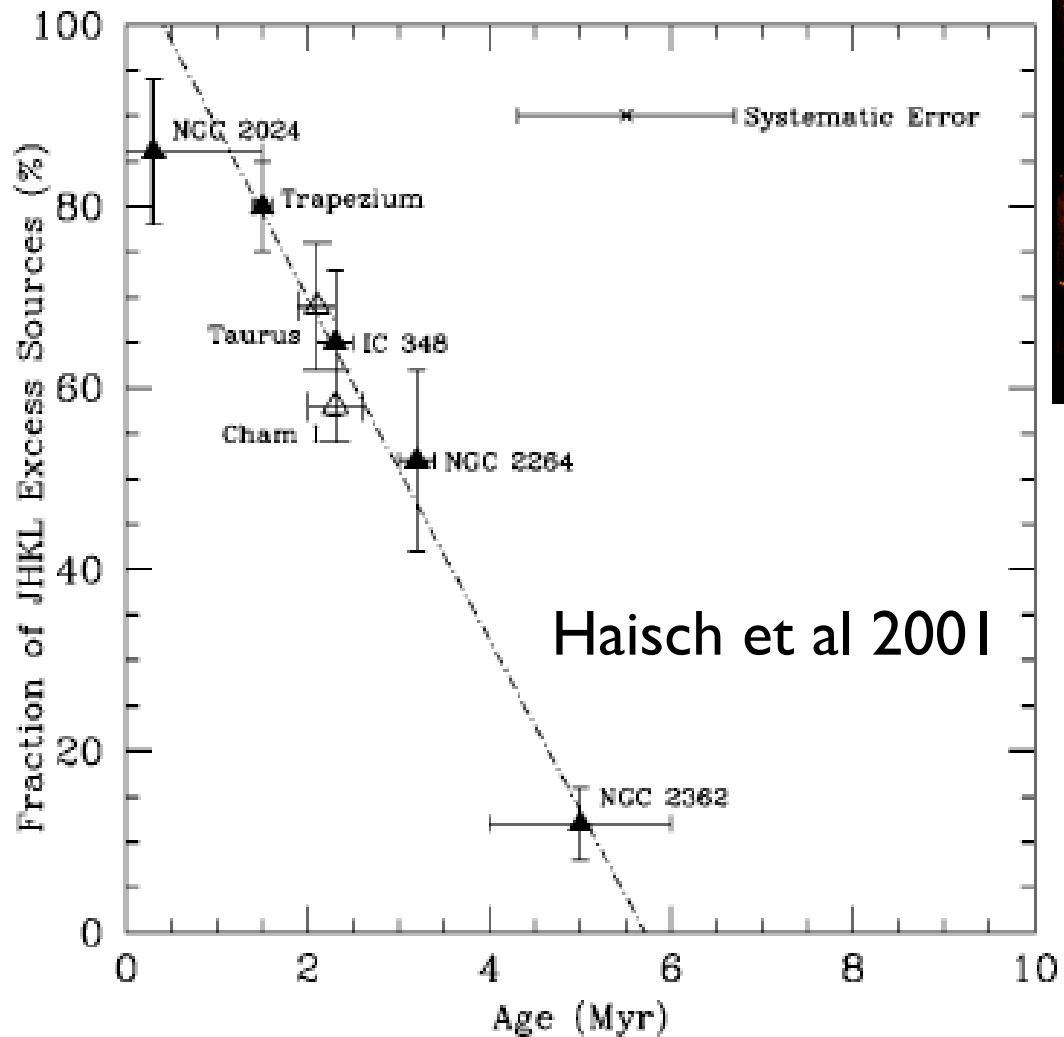
- numerical integration in envelope
- energy deposition into envelope



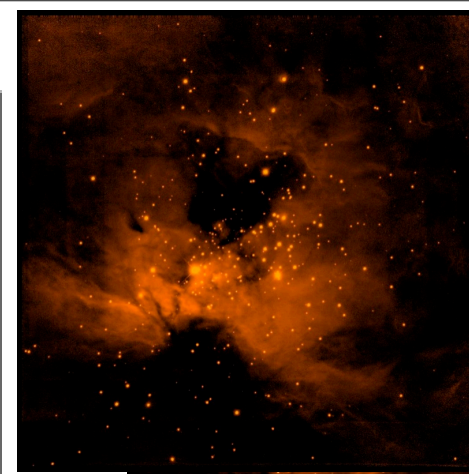
Earth Masses



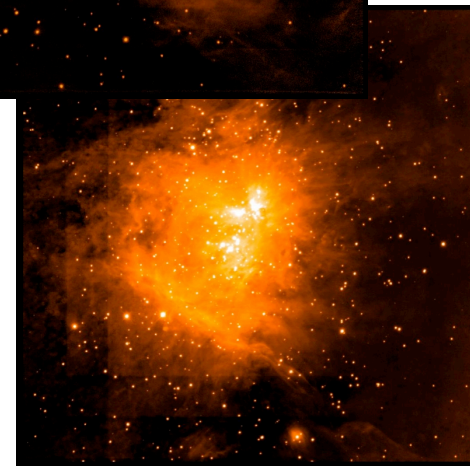
$$d = 5.2 \text{ AU} \quad \sigma_{solids} = 10 \text{ g cm}^{-2}$$
$$T_{neb} = 150 \text{ K} \quad \rho_{neb} = 5 \times 10^{-11} \text{ g cm}^{-3}$$



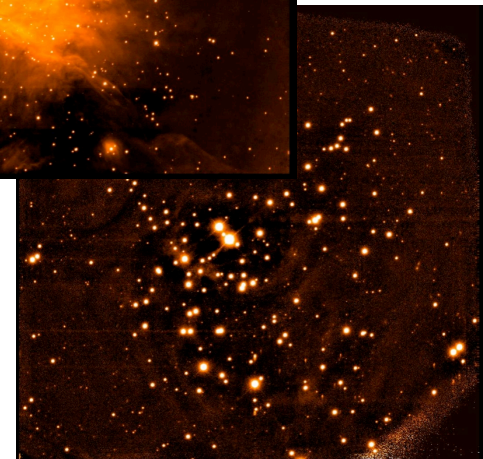
Observed disk lifetimes tend to be in the 2-3 Myr range.



ngc 2024



trapezium



ic 348



ngc 2362

The “standard model” of Pollack et al 1996 predicts:

1. A planet with a core mass that seems too high.
2. A timescale to reach runaway gas accretion that seems too long.

A great deal of work has been done from 1996-2006 to refine core accretion. Examples include:

1. Improved physics:

equation of state (reviewed by Saumon & Guillot 2004)

envelope opacity (Ikoma et al 2000, Podolak 2003)

2. Additional physics:

migration of the cores

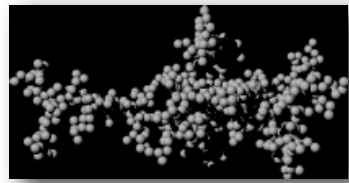
(Papaloizou & Terquem 1999, Alibert et al 2004, Ida & Lin 2004)

turbulence in the disk (Rice and Armitage 2003)

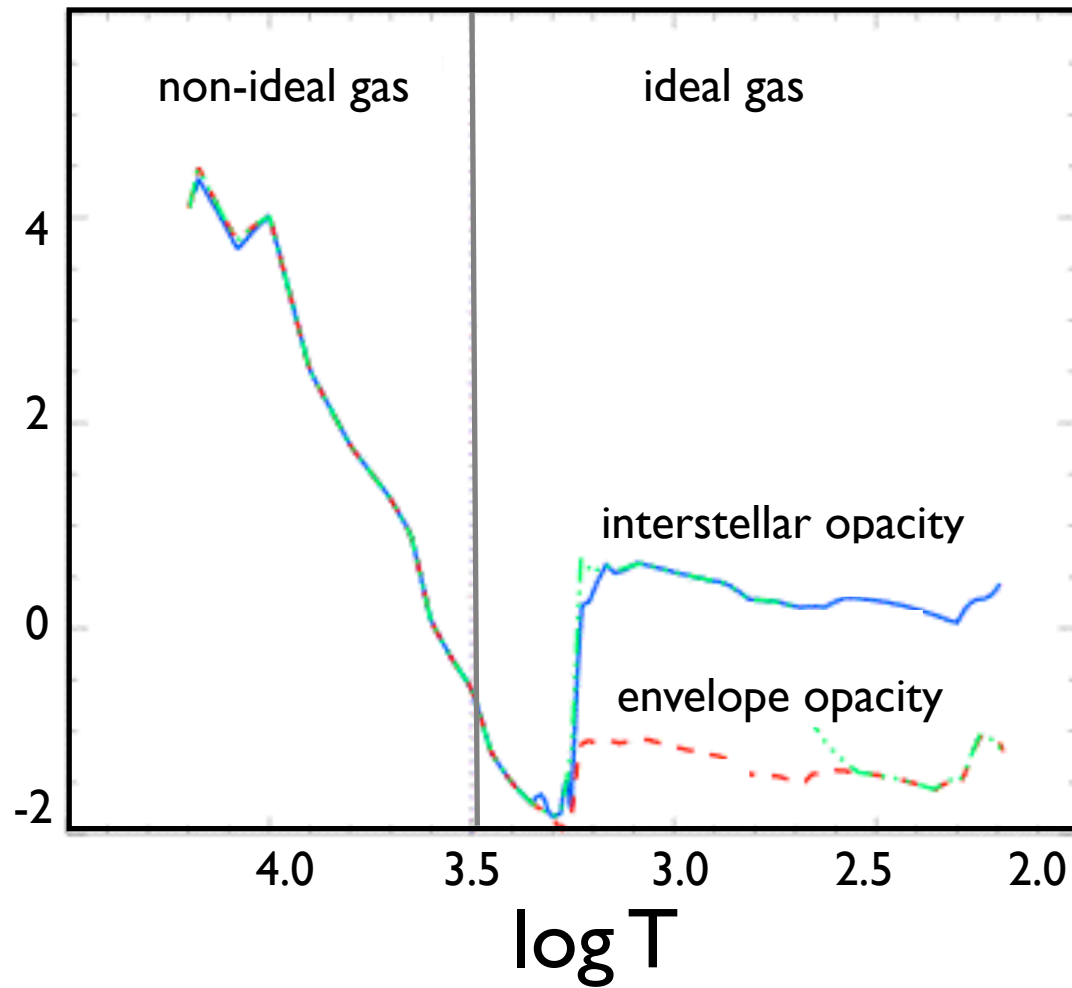
competition between embryos (Hubickyj, Bodenheimer & Lissauer 2005)

time evolution of the disk

(Alibert et al 2004, Ida & Lin 2004, Laughlin, Bodenheimer & Adams)

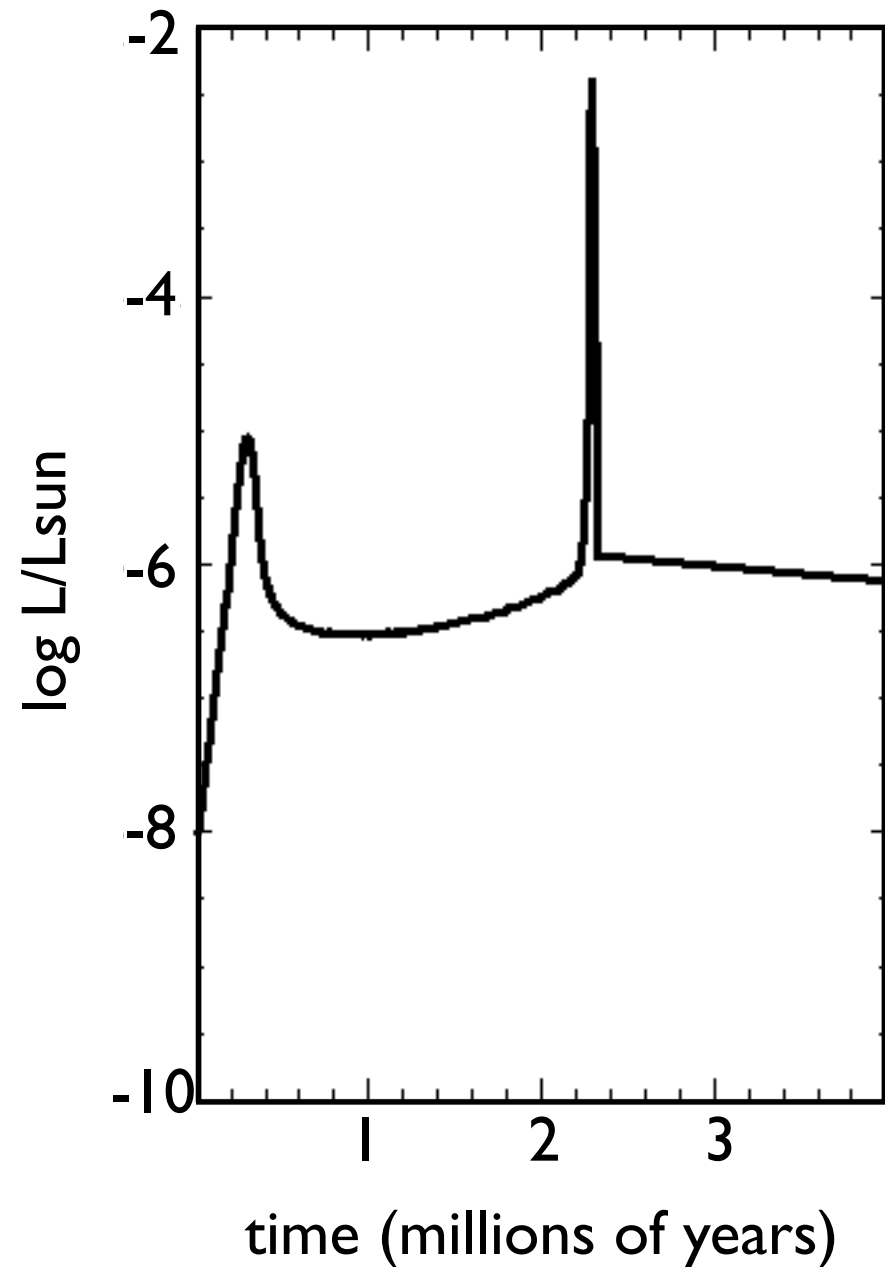
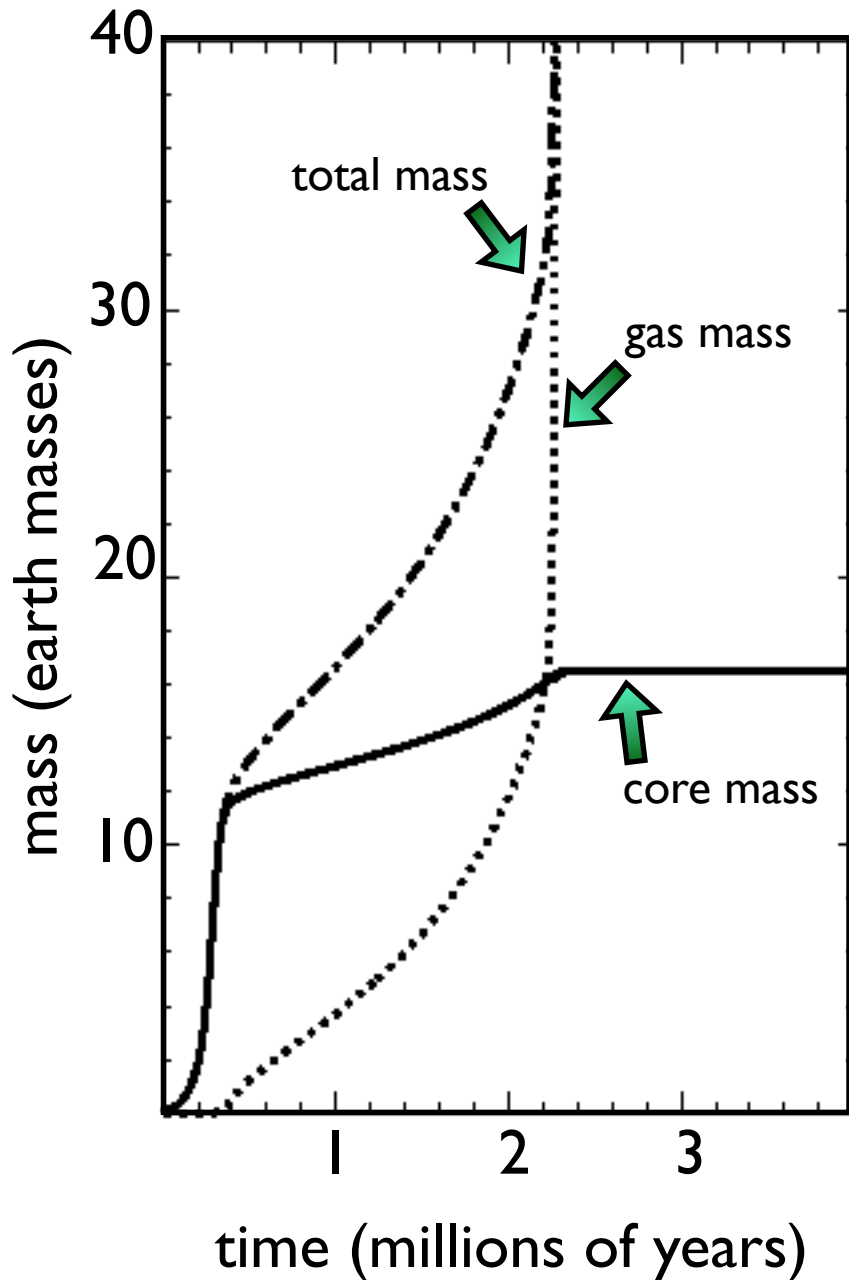


$\log \kappa$



- Grain opacities are a key issue. Original studies (e.g Pollack et al 1996) used envelope opacities with an interstellar size distribution.
- But material that enters a giant planet envelope has been modified from the original interstellar grains by coagulation and fragmentation.
- Calculations by Podolak (2003) indicate that once grains enter the protoplanetary envelope, they coagulate and settle out quickly into warmer regions where they are destroyed. Podolak argues that true opacities are $\sim 50x$ smaller than interstellar.

Reduced grain opacity greatly speeds up the gas accretion timescale.

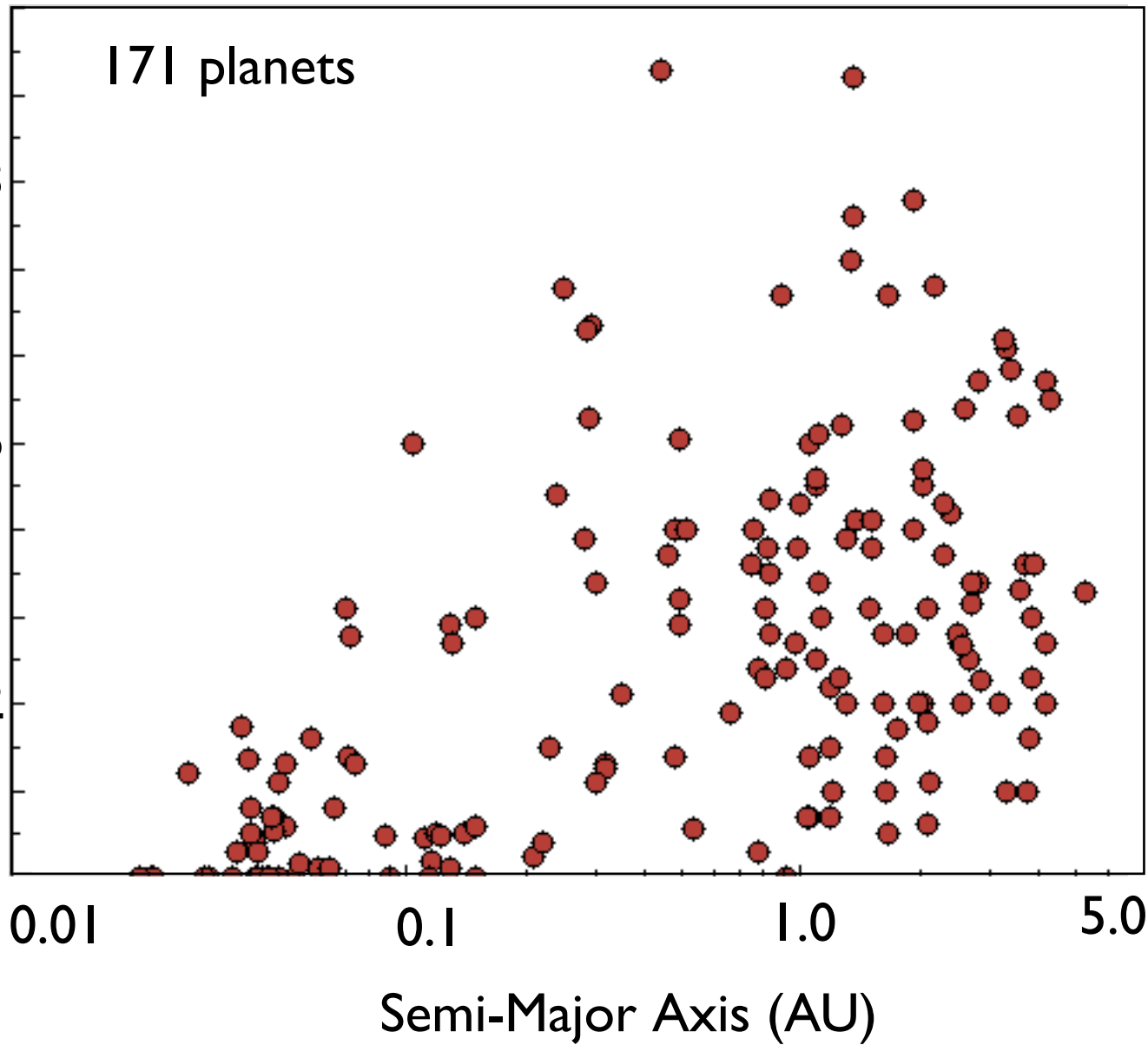
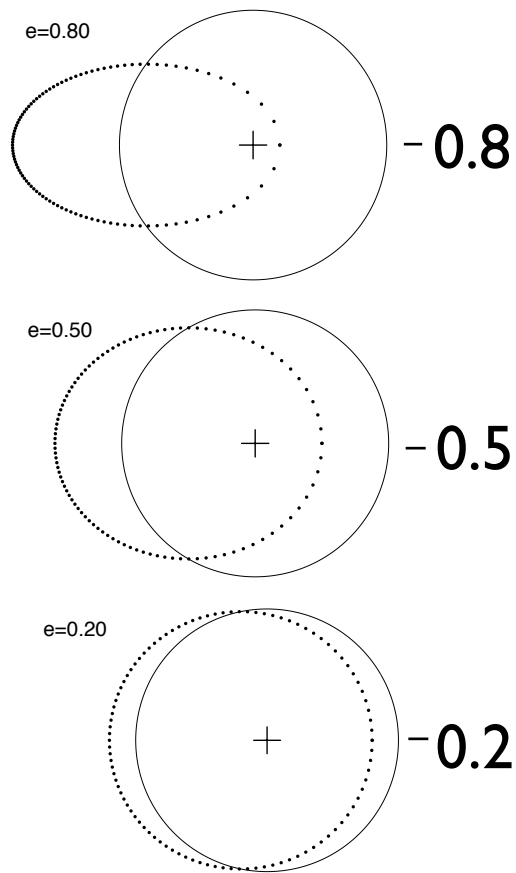


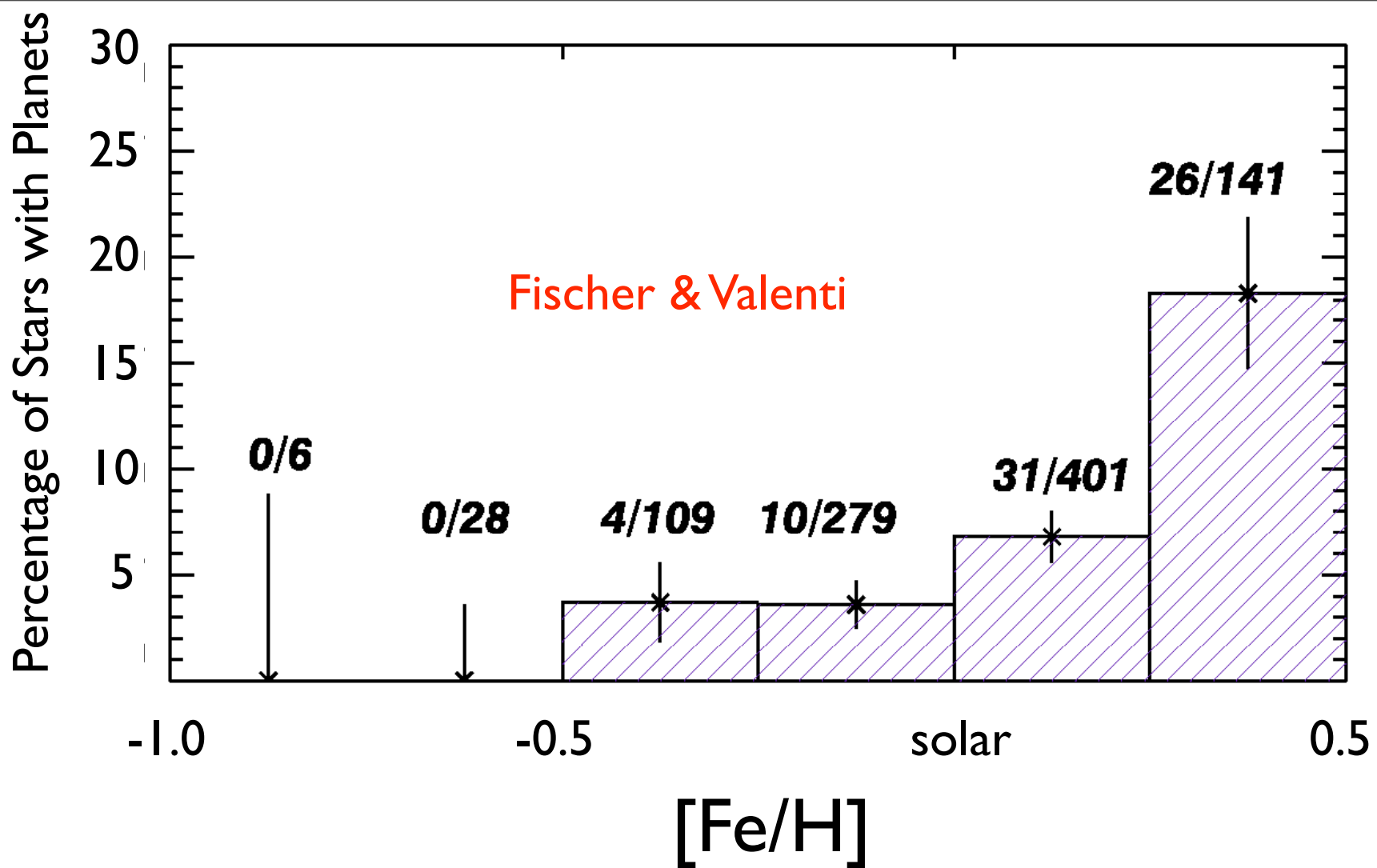
(Hubickyj et al. 2005)

A key (and well established) result of standard core accretion theory is the extraordinary sensitivity of the time of onset of rapid gas accretion to the surface density of solids in the disk.

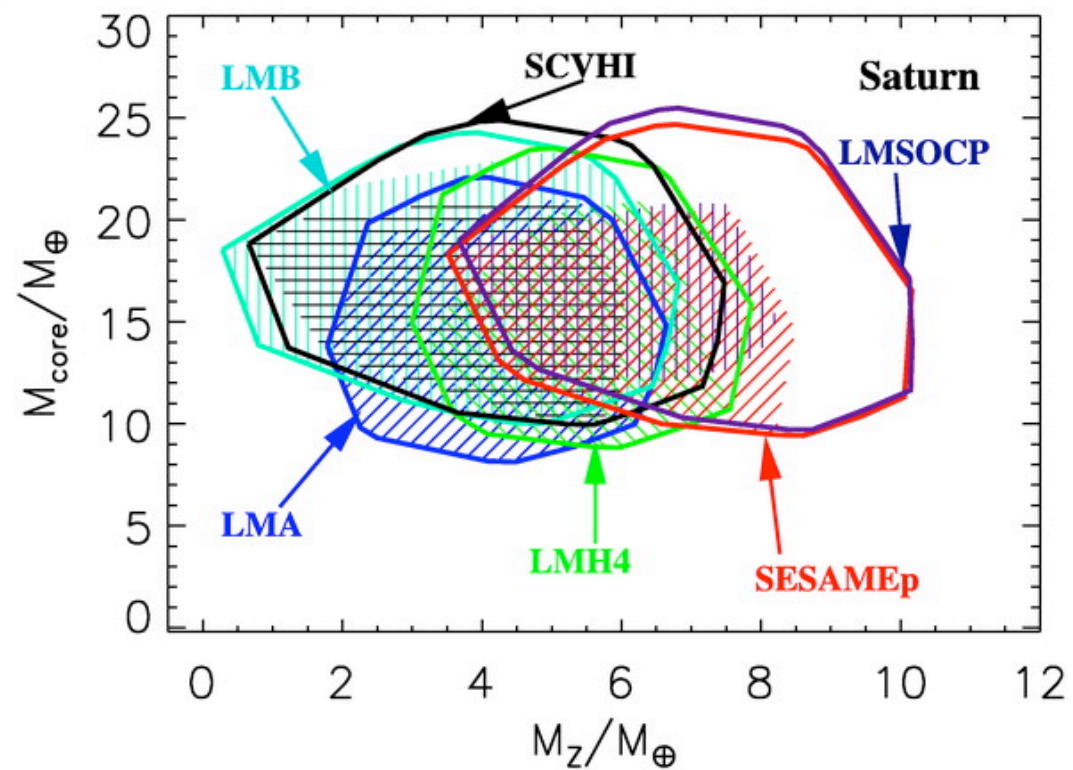
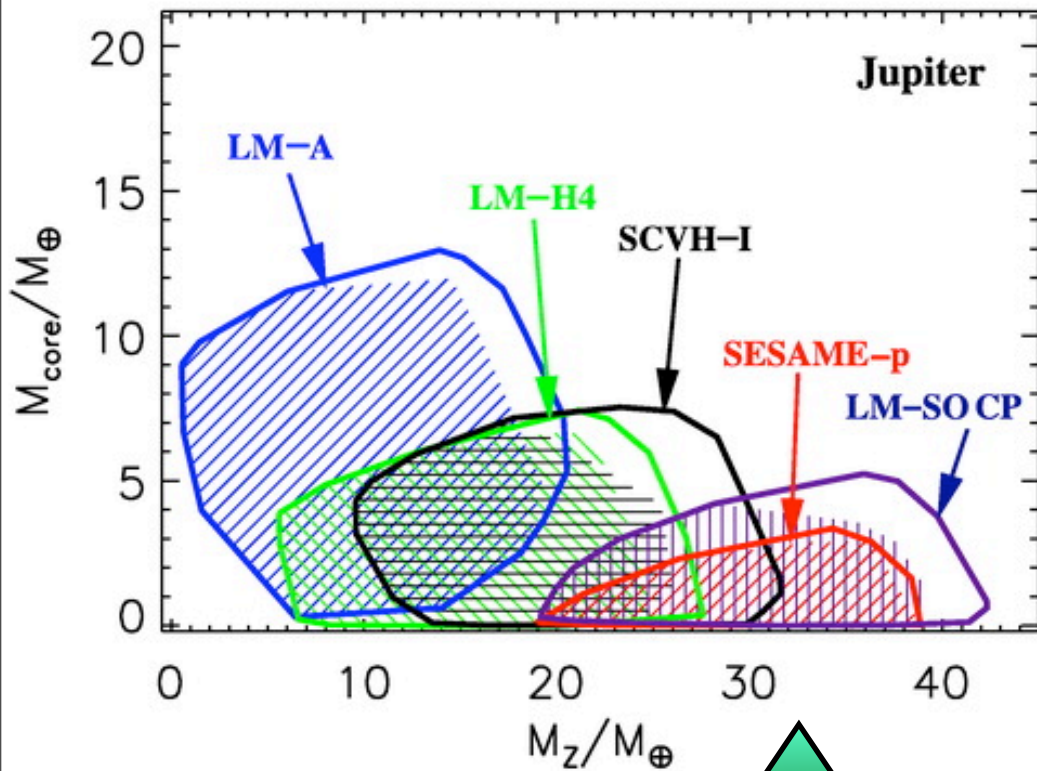
Recent calculations by Hubickyj et al (2005), illustrate that decreasing the solid surface density from 10 to 6 gm/cm² causes a 12 Myr delay in the onset of rapid gas accretion.

orbital eccentricity





The extrasolar planet - host star metallicity connection is one of the most remarkable results to have emerged from the radial velocity surveys. This correlation certainly provides an important clue to the planet formation process.



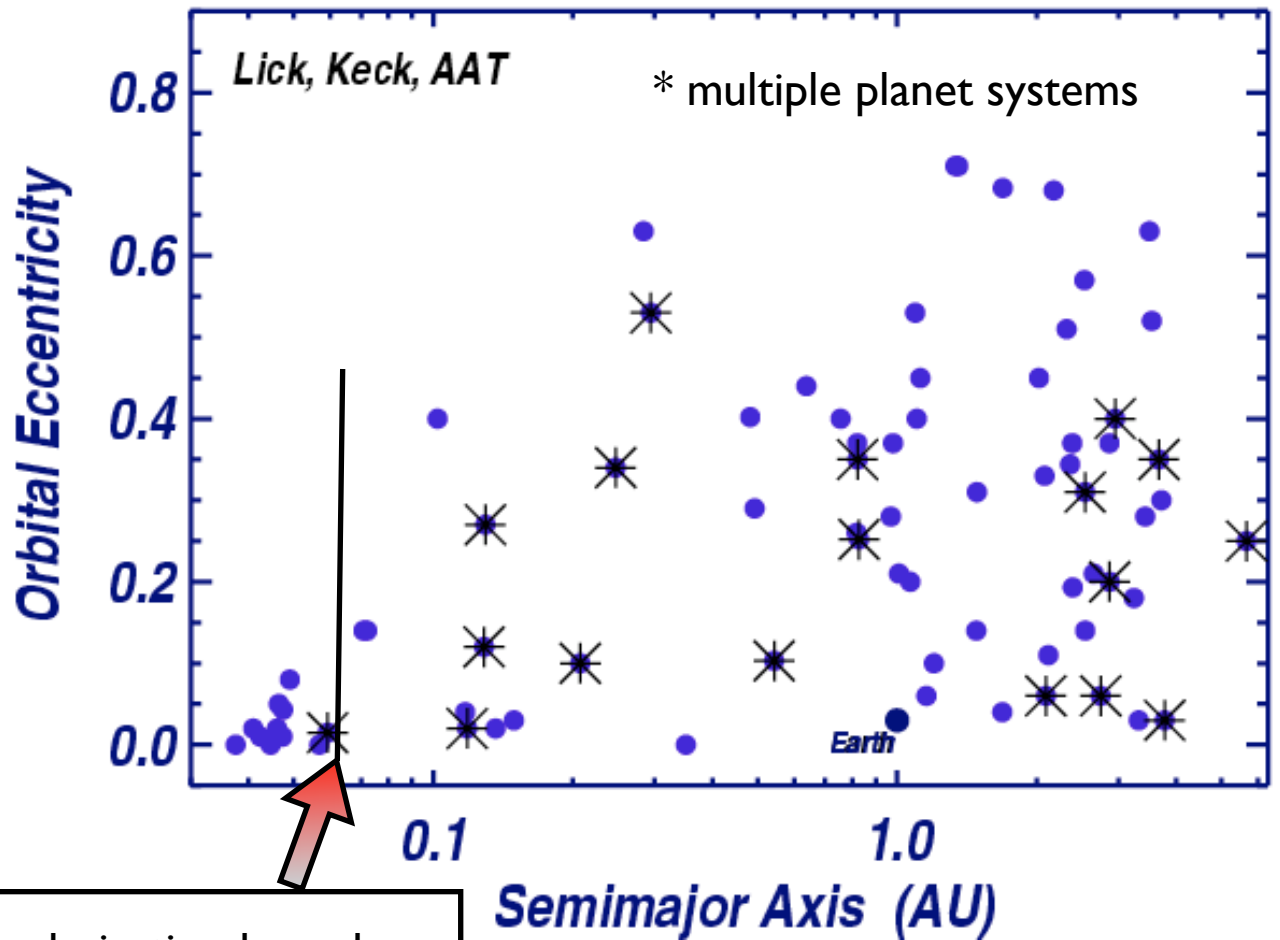
Saumon and Guillot (2004) compute the allowed ranges for Jupiter's core mass and the mass of heavy elements mixed into the envelope for which planetary models having different different H-He equations of state can match Jupiter's R_{eq} , J_2 and J_4 to 2-sigma.

Jupiter seems to have a small core.

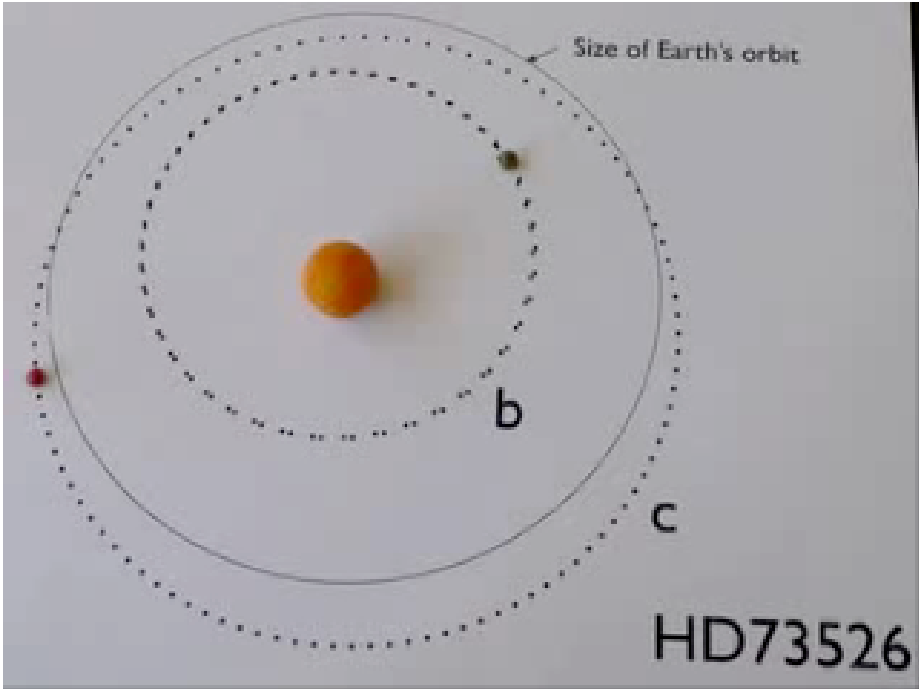
As more planets with periods of approximately one week are discovered, the tidal quality factor, Q , which in general should depend on Mass, T_{eff} , and composition will become better constrained. Right now, the circularization boundary suggests

$$\langle Q \rangle \sim 10^6$$

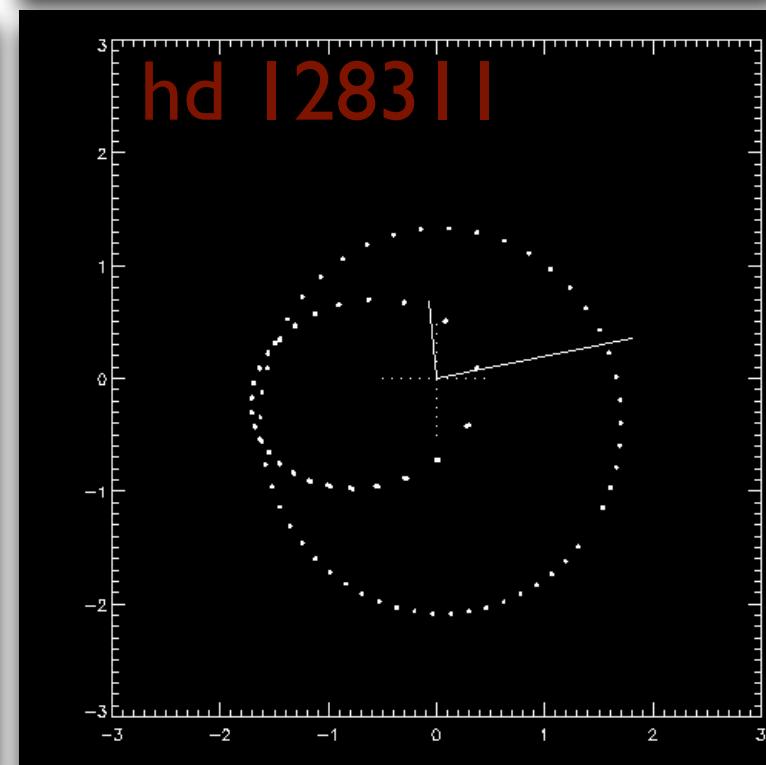
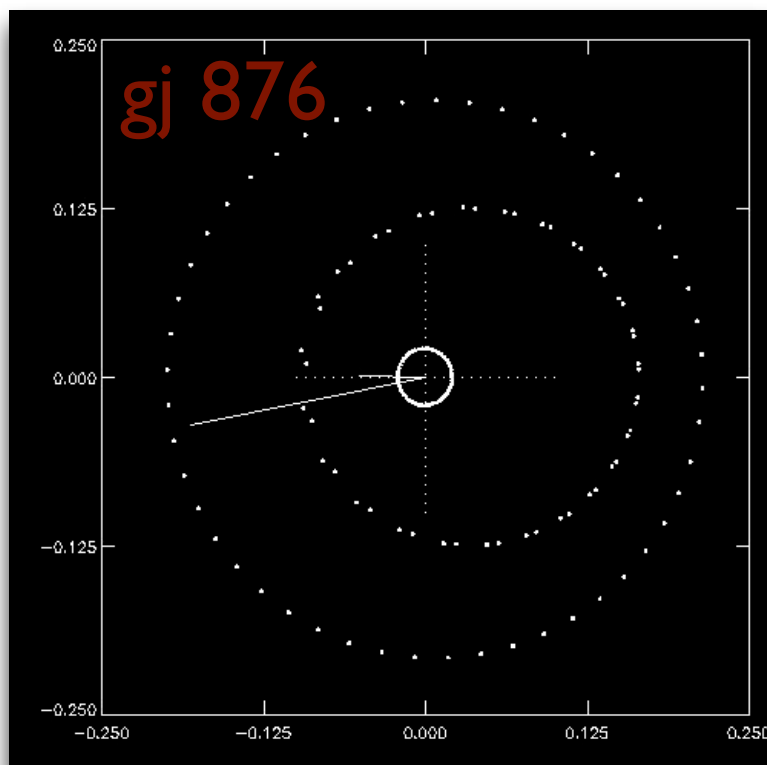
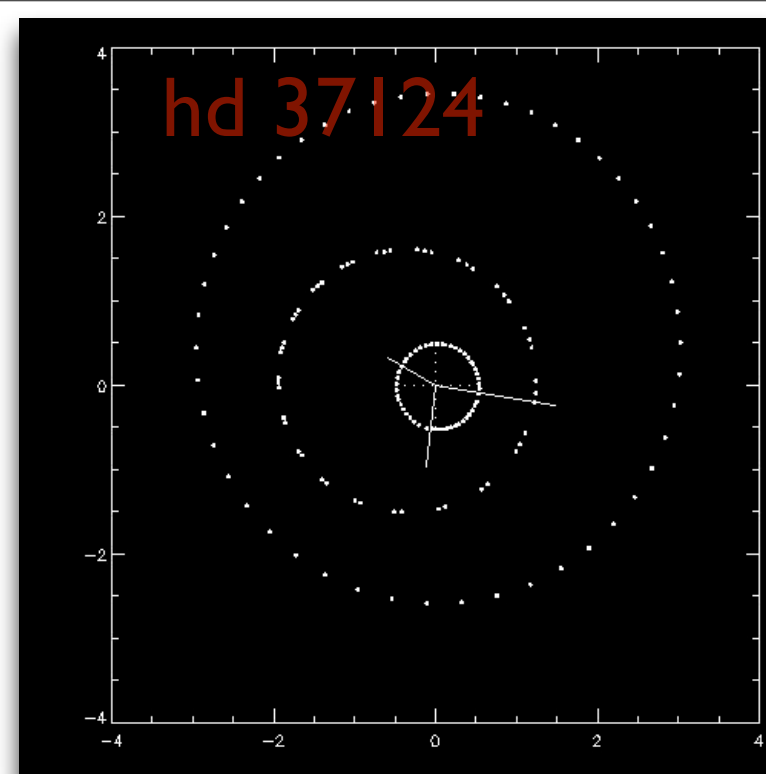
circularization boundary occurs at a period of about one week.



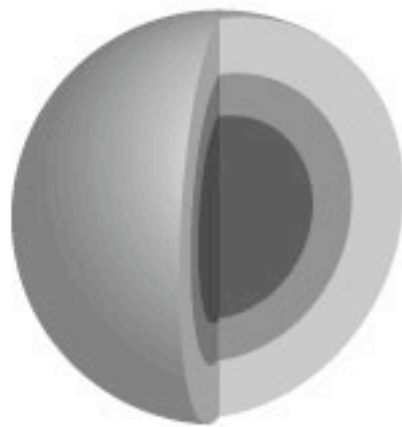
$$\tau_{\text{circ}} = \frac{e}{\dot{e}} = \left(\frac{4Q_P}{63n} \right) \left(\frac{M_P}{M_\star} \right) \left(\frac{a}{R_p} \right)^5$$



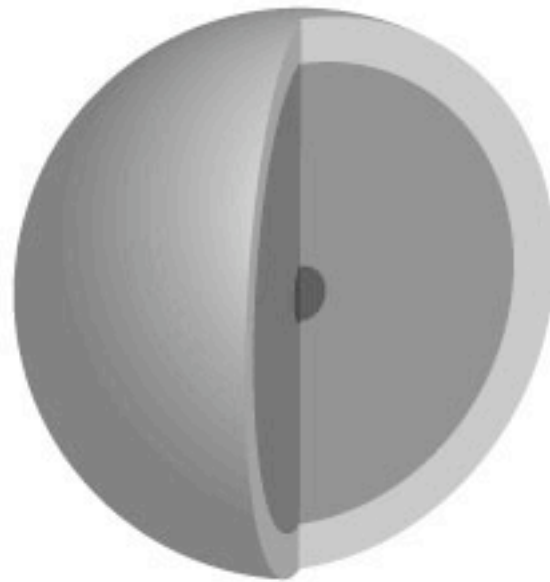
Over half of the short-period planets that have been discovered show evidence for detectable additional companions. Multiple-planet systems can tell us much more about the formation and evolutionary processes that are sculpting the galactic planetary census.



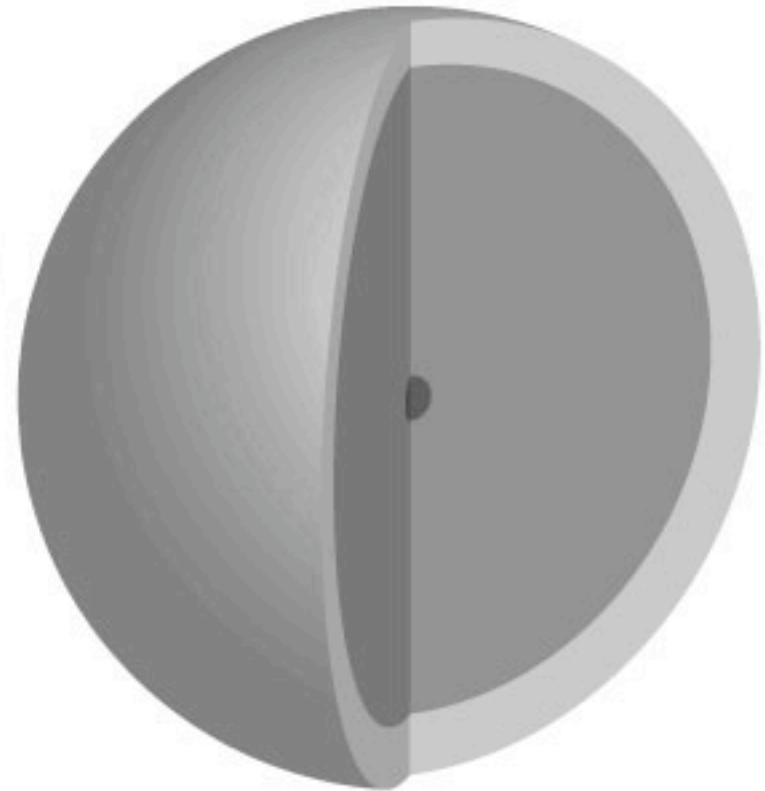
The size of HD 209458b, HD 149026b, and the other known transiting planets show that there are a large range of core masses.



HD 149026 b



Jupiter



HD 209458 b



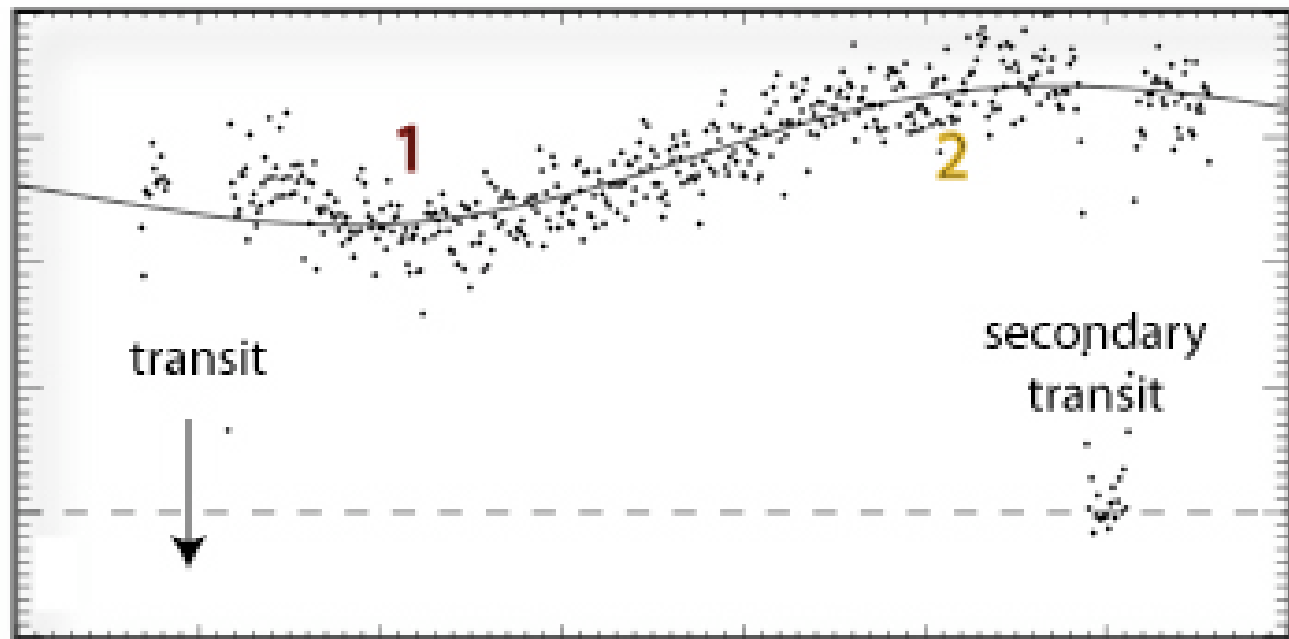
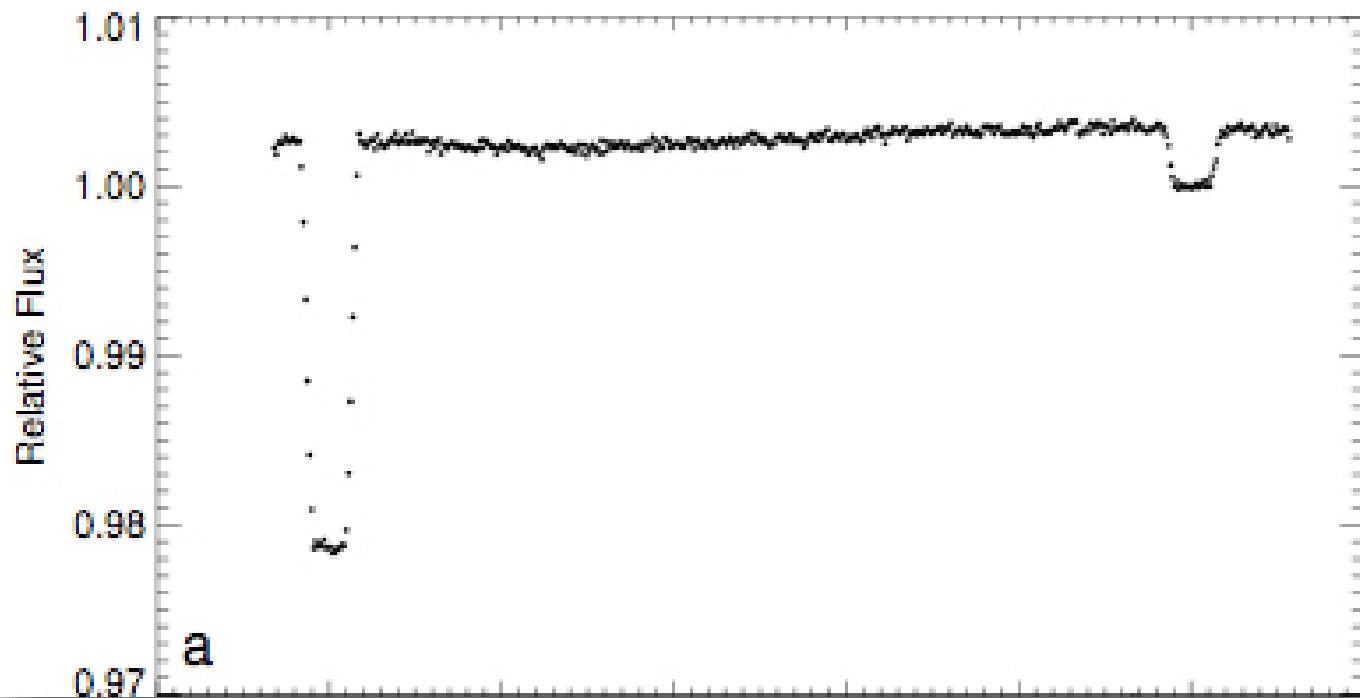
Neptune

deep hydrogen-enriched atmosphere
heavy element core

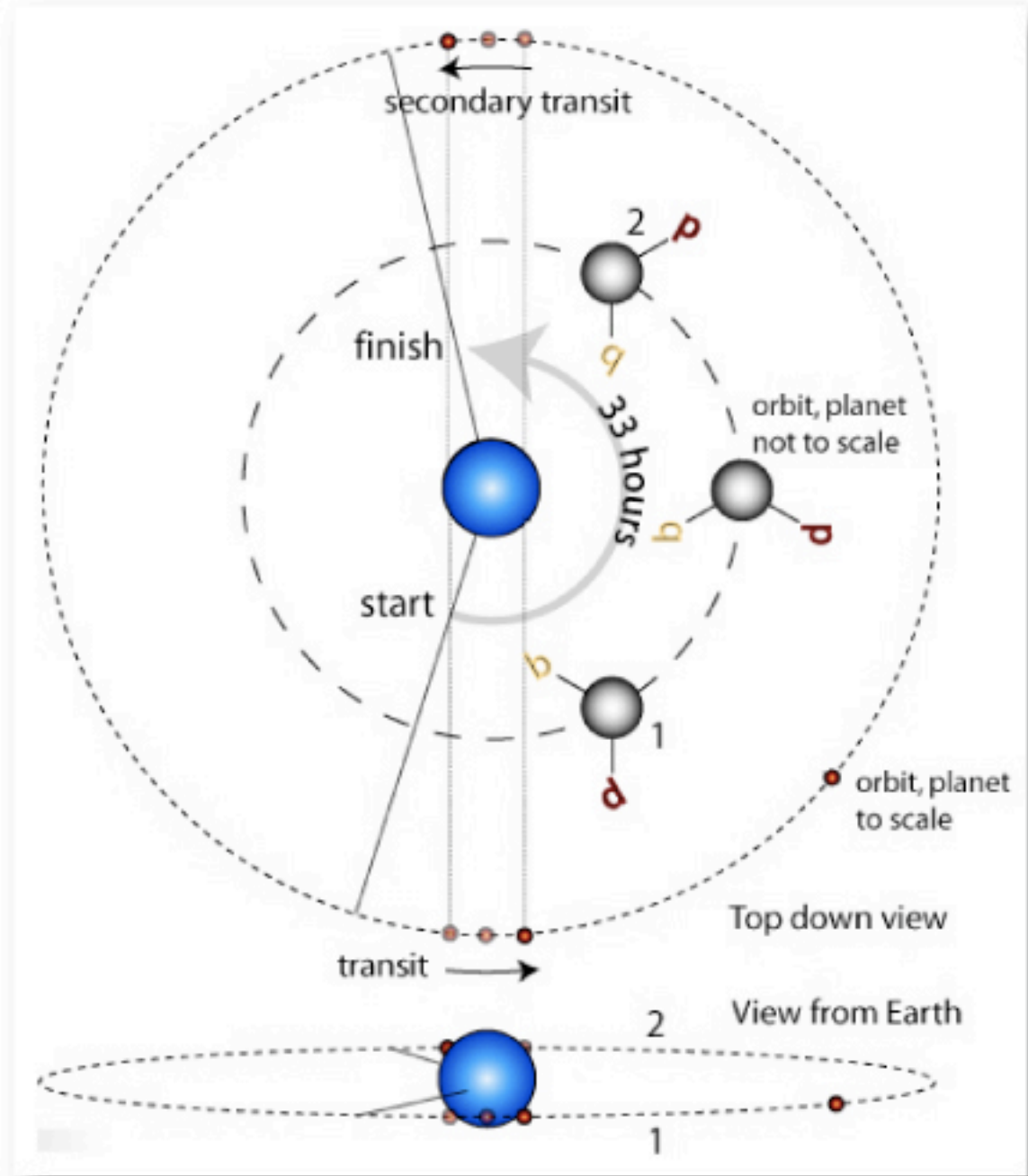
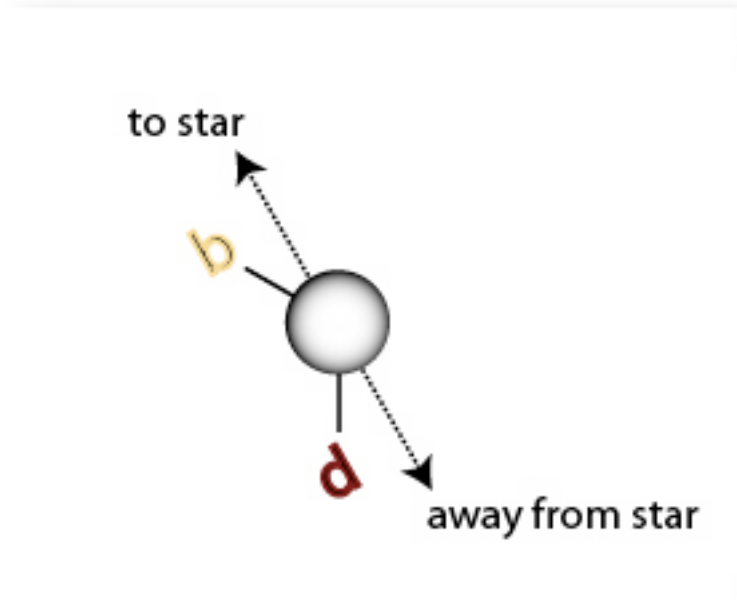
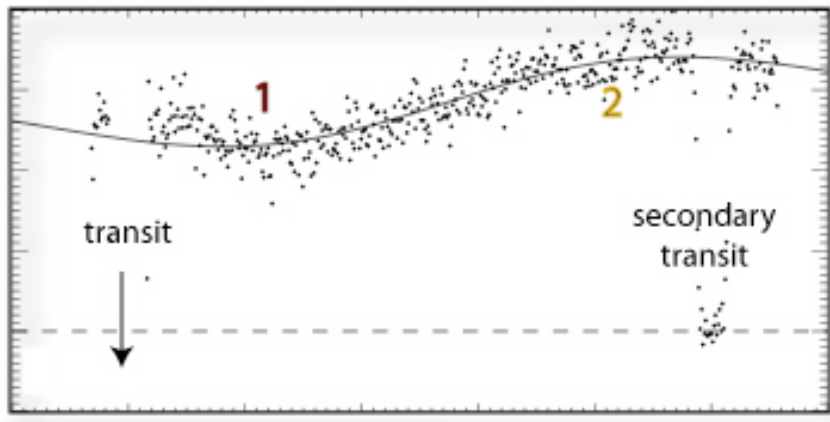
- light grey box: molecular hydrogen and helium
- medium grey box: liquid metallic hydrogen
- dark grey box: heavy element core

	Planet		Orbit				R
	Mpl [M _J]	Rpl [R _J]	P [days]	Ttr [JD-2450000]	i [°]	a [AU]	
<i>OGLE-TR-10</i>	0.61 (0.13)	1.122 (+0.12-0.07)	3.101278 (_4)	3890.678 (_1)	87.2-90	0.04162 (0.00069)	[Konacki05]Pont0
<i>OGLE-TR-56</i>	1.29 (0.12)	1.30 (0.05)	1.211909 (_1)	3936.598 (_1)	81.0 (2.2)	0.0225 (0.0004)	[K03]Torres04/Po
<i>OGLE-TR-111</i>	0.52 (0.13)	1.01 (0.04)*	4.0144479 (_41)	3799.7516 (_2)	88.1 (0.5)	0.0467 (0.005)	[Pont04]Santos06
<i>OGLE-TR-113</i>	1.32 (0.19)	1.09 (0.03)	1.4324757 (_13)	3464.61665(_10)	88.8-90	0.0229 (0.0002)	[Bouchy04]Bouch
<i>OGLE-TR-132</i>	1.14 (0.12)	1.18 (0.07)	1.689868 (_3)	3142.5912 (_3)	81.5 (1.6)*	0.0299*	[Bouchy04]Gillon
<i>HD189733</i>	1.15 (0.04)	1.156 (0.046)	2.2185733 (_19)	3988.80336 (_23)	85.76 (0.29)	0.031 (0.001)	[Bouchy05]Winn0
<i>HD149026</i>	0.330 (0.02)	0.726 (0.064)	2.87598 (_15)	3527.87455 (_90)	85.8 (+1.6-1.3)	0.042	[Sato05]Charbonn
<i>TrES-1</i>	0.76 (0.05)	1.081 (0.029)	3.0300737 (_26)	3186.80603 (_28)	>88.4	0.0393 (0.0011)	[Alonso04]Sozett
<i>TrES-2</i>	1.198 (0.053)	1.220 (+.045-.042)	2.47063 (_1)	3957.6358 (_10)	83.90 (0.22)	0.0367 (+_12-_05)	[ODonovan06] So
<i>TrES-3</i>	1.92 (0.23)	1.295 (0.081)	1.30619 (_1)	4185.9101 (_3)	8215 (0.21)	0.0226 (0.0013)	[ODonovan07]
<i>HD209458</i>	0.657 (0.006)	1.320 (0.025)	3.52474859 (_38)	2826.628521 (_87)	86.929 (0.010)	0.047 (+.001-.003)	[Charbonneau00]
<i>XO-1</i>	0.90 (0.07)	1.184 (+.028-.018)	3.941534 (_27)	3887.74679 (_15)	89.36 (+.46-.53)	0.0488 (0.0005)	[McCullough06]H
<i>XO-2</i>	0.98 (0.02)	0.964 (+.02-.009)	2.615838 (_8)	4147.74902 (_20)	>88.35		[Burke07]
<i>HAT-P-1</i>	0.53 (0.04)	1.36 (+.11-.09)	4.46529 (_9)	3984.397 (_9)	85.9 (0.8)	0.0551 (0.0015)	[Bakos07]
<i>HD147506</i>	8.17 (0.72)	1.18 (0.16)	5.63341 (_13)	4212.8561 (_23)	90.0 (1.0)	0.0685 (0.0017)	[Bakos07]
<i>WASP-1</i>	0.867 (0.073)	1.443 (0.039)	2.519961 (_18)	4013.31269 (_47)	>86.1	0.0382 (0.0013)	[Cameron06]Shpo
<i>WASP-2</i>	0.81-0.95	1.038 (0.050)	2.152226 (_4)	4008.73205 (_28)	84.74 (0.39)	0.0307 (0.0011)	[Cameron06]Char
<i>GJ436</i>	0.071 (0.006)	0.35 (0.03)	2.64385 (_9)	4222.616 (_1)	86.5 (0.2)	0.028 (0.001)	[Gillon07]

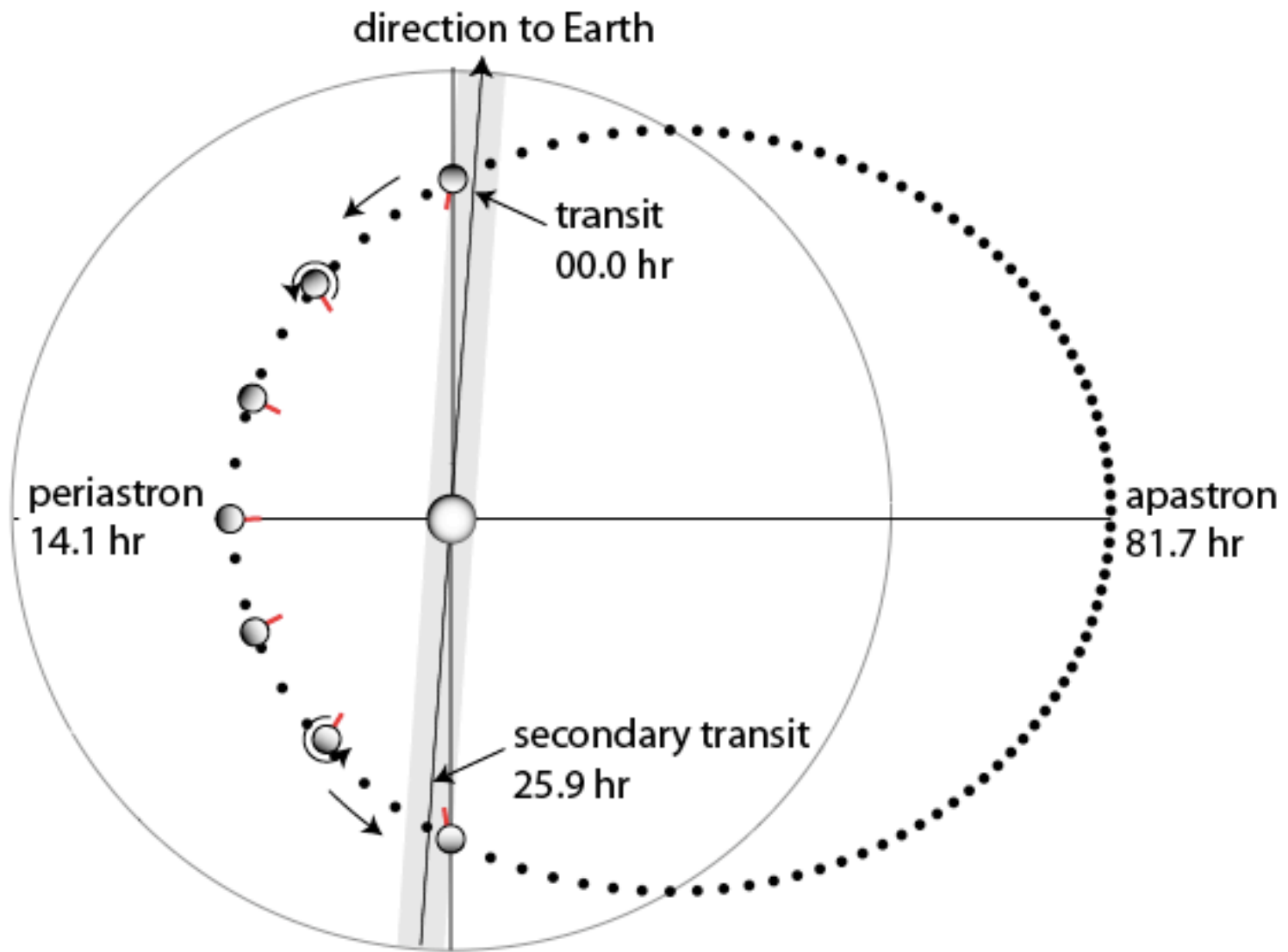
Frederic Pont's Summary Table of 18 Transiting Planets



Incredible follow-up observations are being made with Spitzer. These observations of HD 189733 come from Knutson et al. 2007.

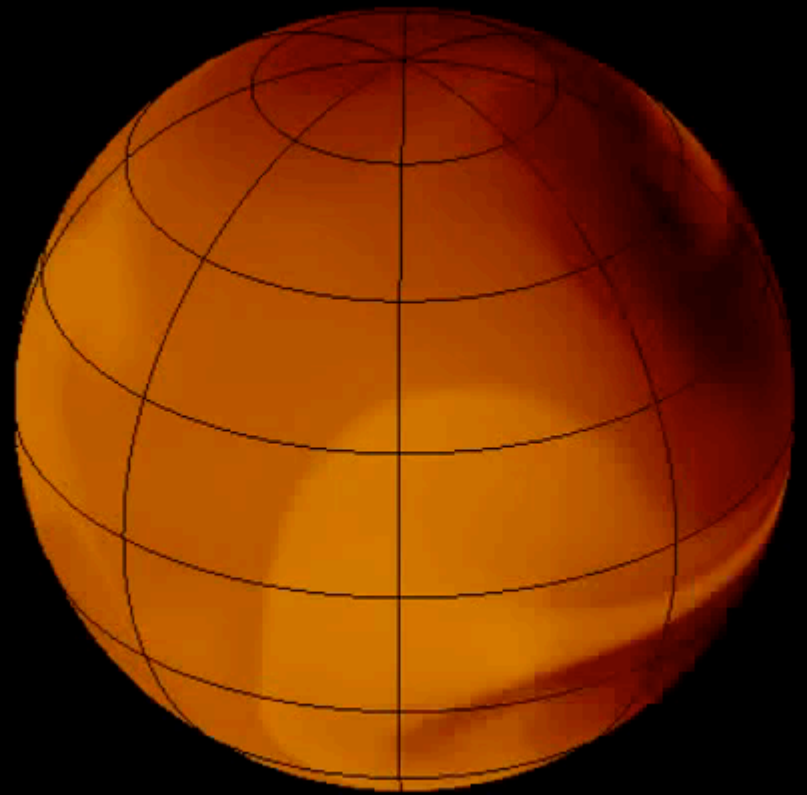
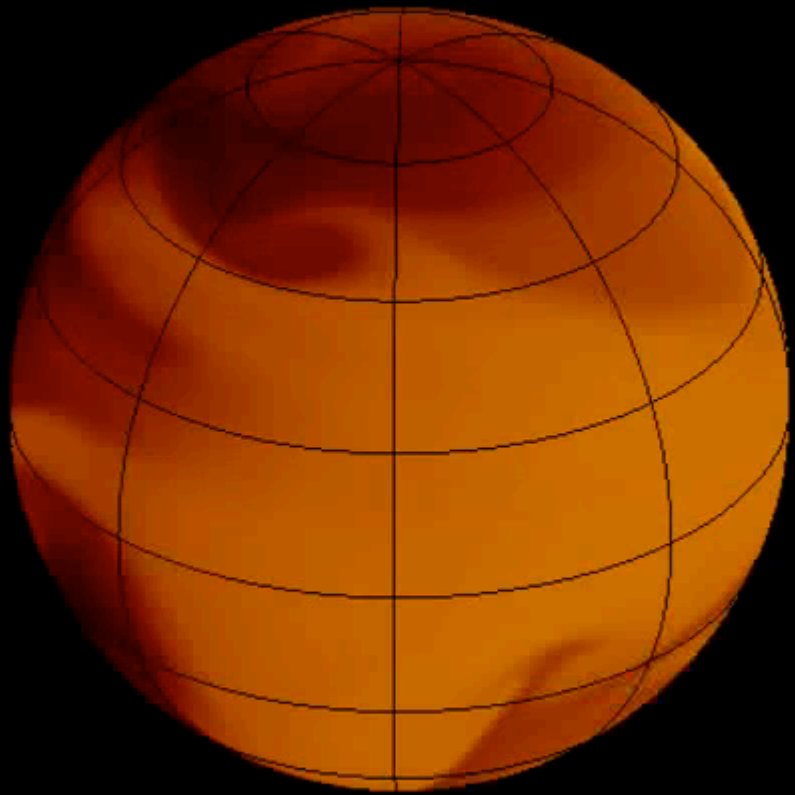


Interpretation of the result: Hottest and coldest spots are on the same side of the planet.

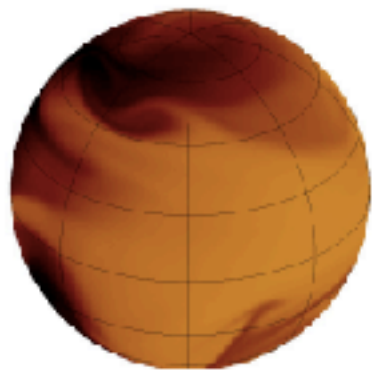


HAT-P-2b

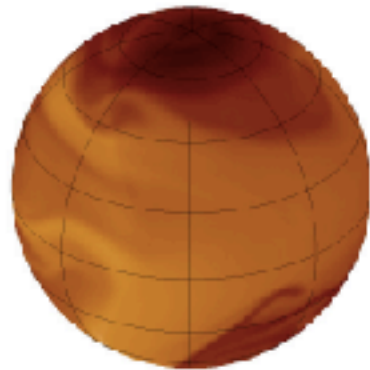
HAT-P-2b



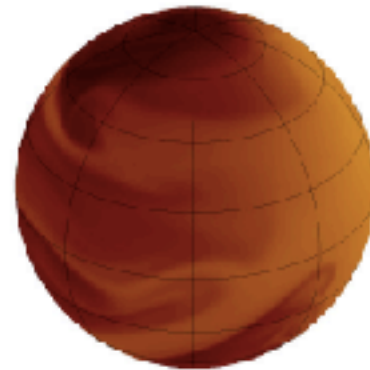
Temperature Range: 950K to 2170K



0.00 hr
(apastron)



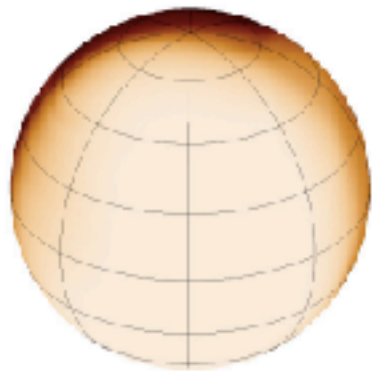
19.2 hr



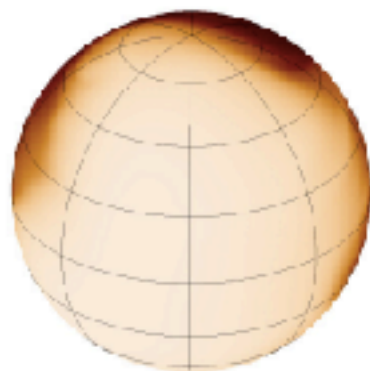
38.4 hr



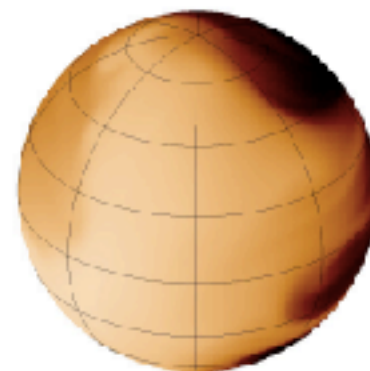
76.8 hr



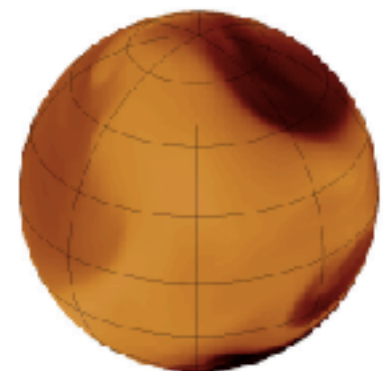
96.0 hr



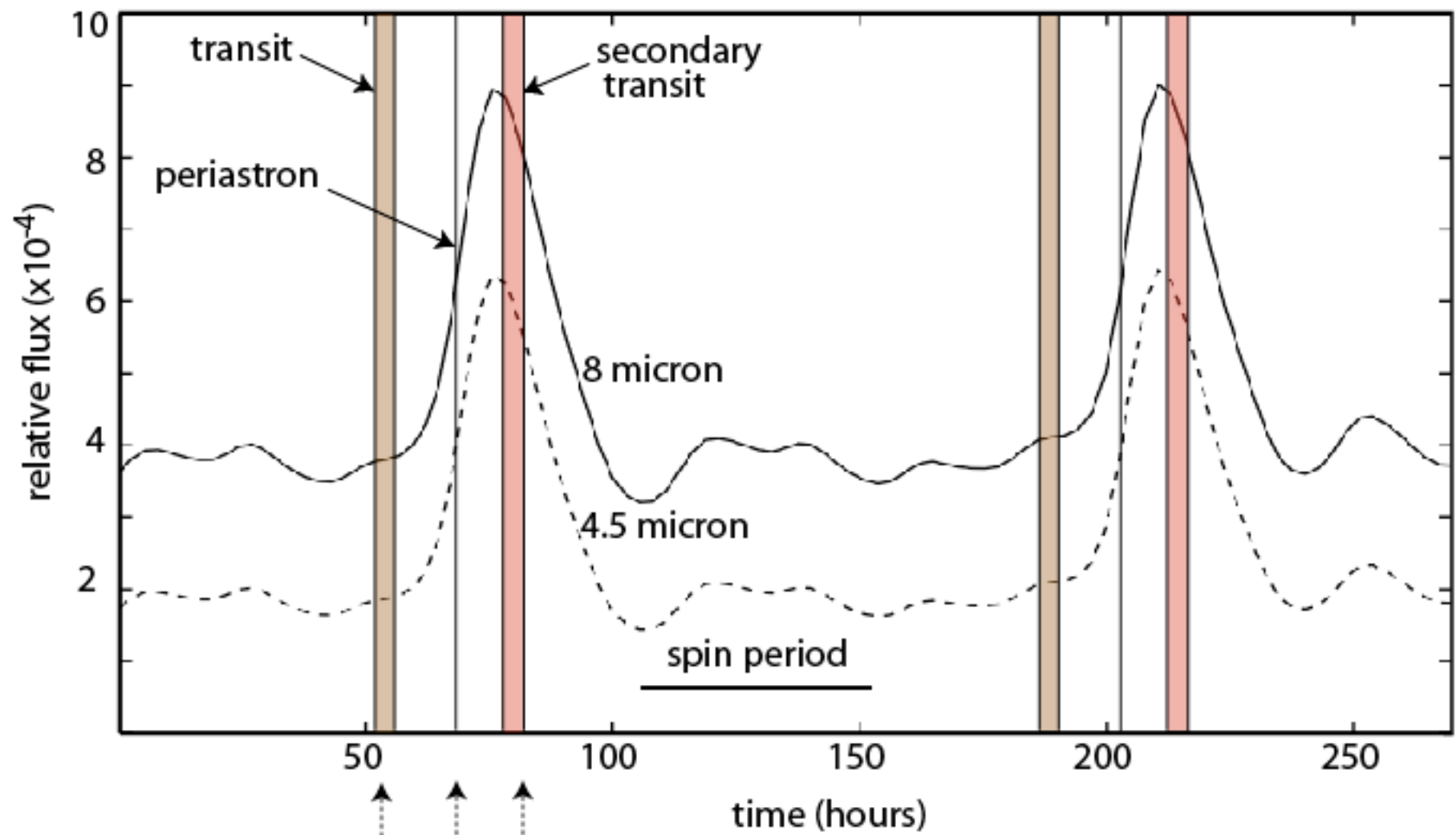
115.2 hr



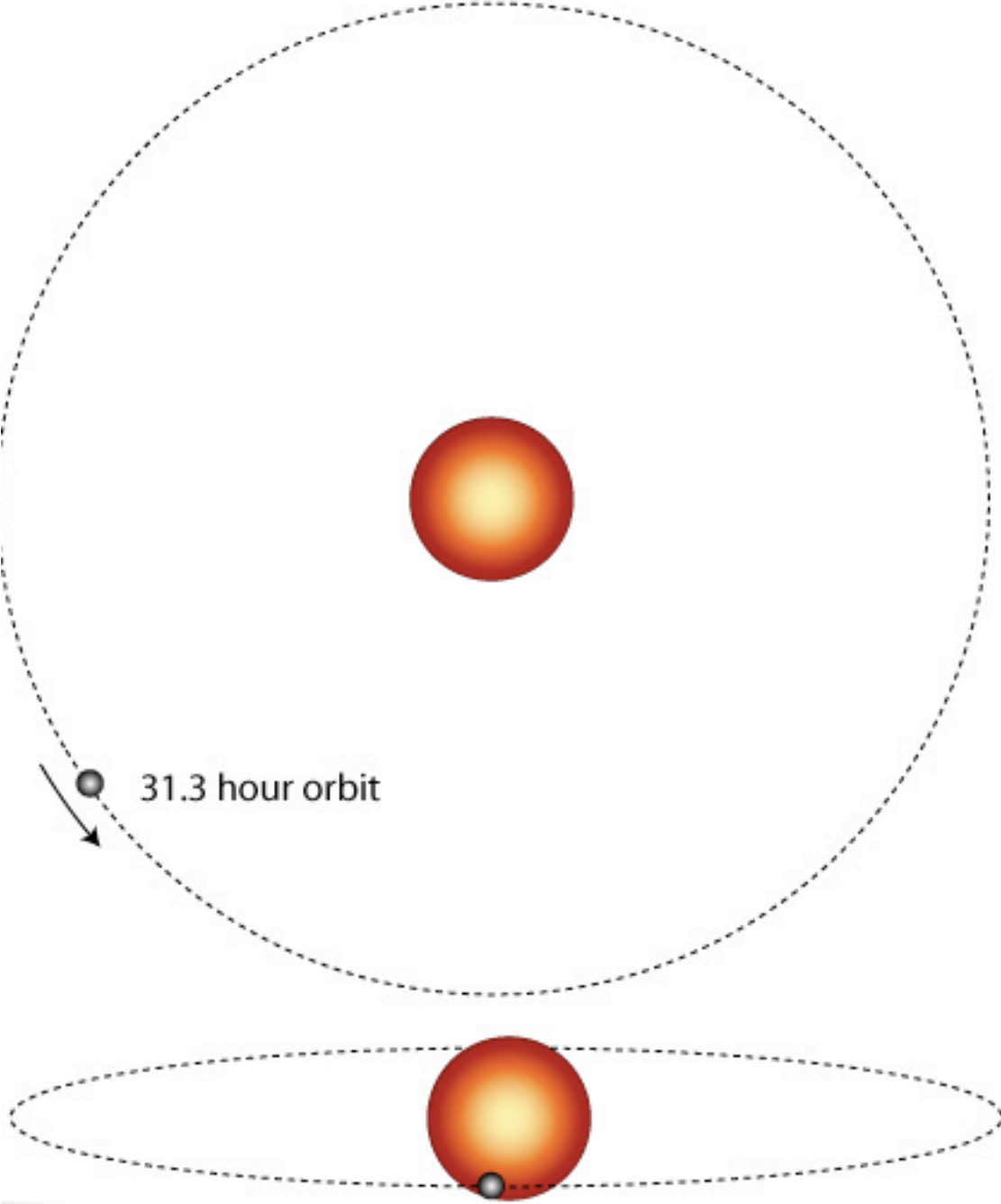
134.4 hr



153.6 hr



TrES-3b to Scale



A great deal of work has been done in the last decade to refine core accretion. Examples include:

1. Improved physics:

equation of state (reviewed by Saumon & Guillot 2004)

envelope opacity (Ikoma et al 2000, Podolak 2003, Marley et al. 2006)

2. Additional physics:

migration of the cores

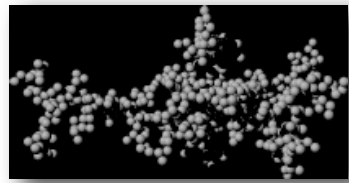
(Papaloizou & Terquem 1999, Alibert et al. 2004, 2006, Ida & Lin 2004, 2006)

turbulence in the disk (Rice and Armitage 2003)

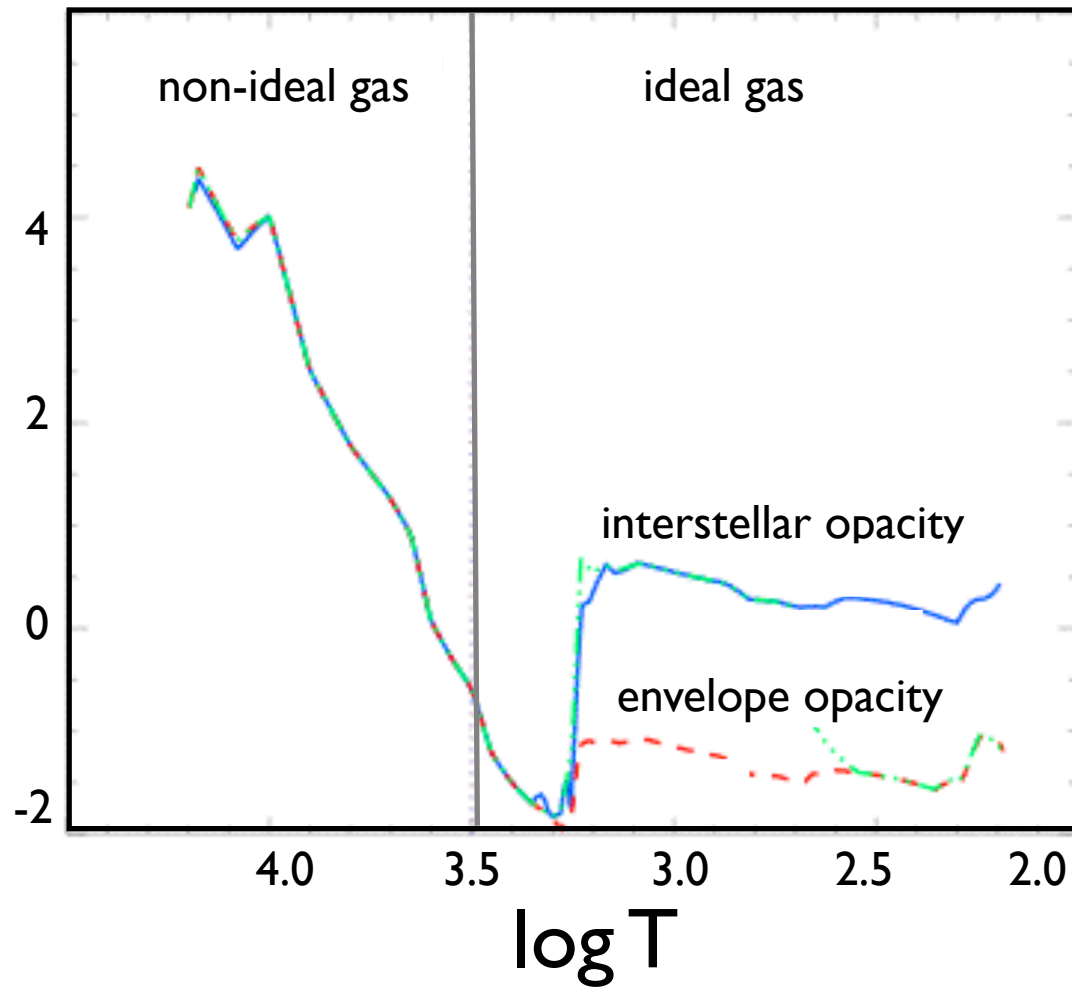
competition between embryos (Hubickyj, Bodenheimer & Lissauer 2005)

time evolution of the disk

(Alibert et al. 2005, 2006, Ida & Lin 2004, Laughlin, Bodenheimer & Adams 2004)

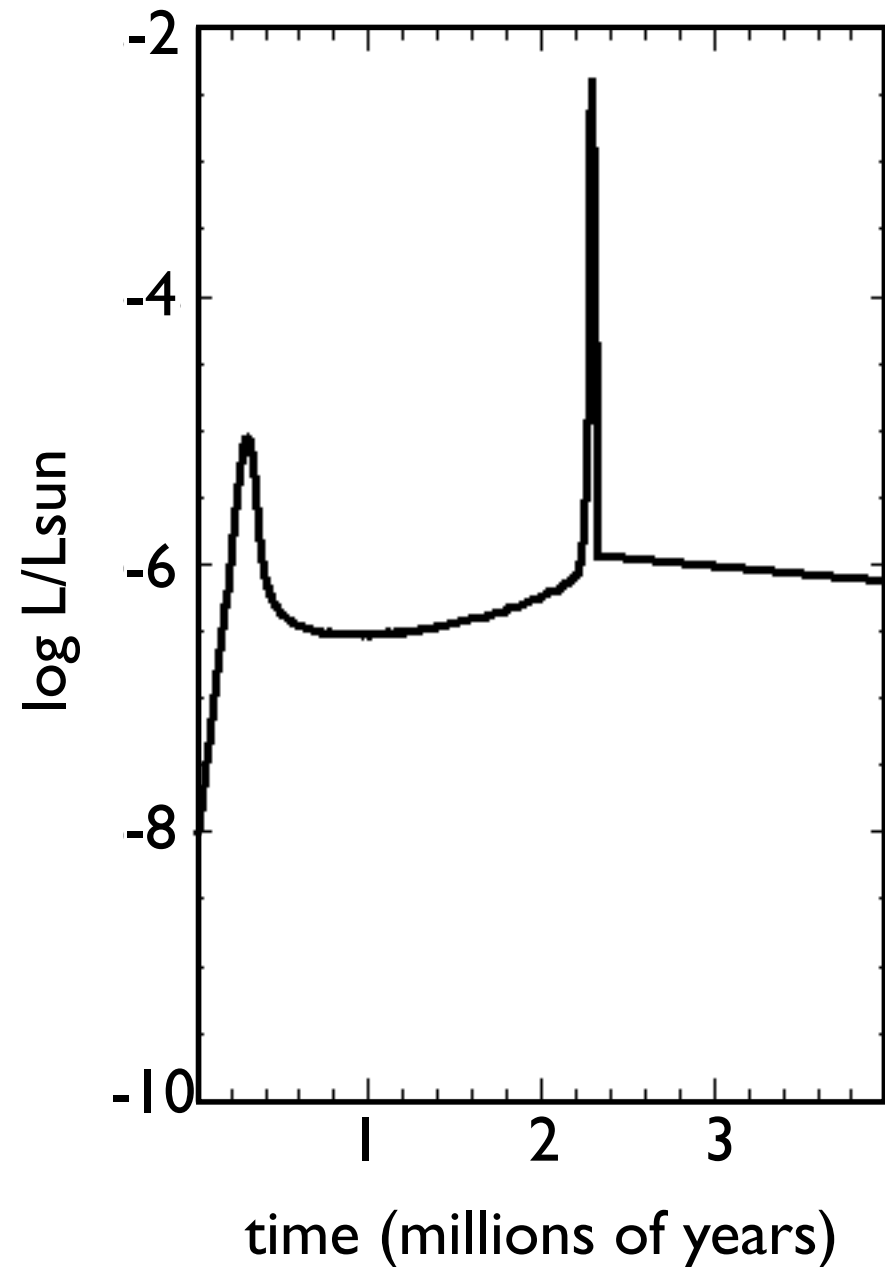
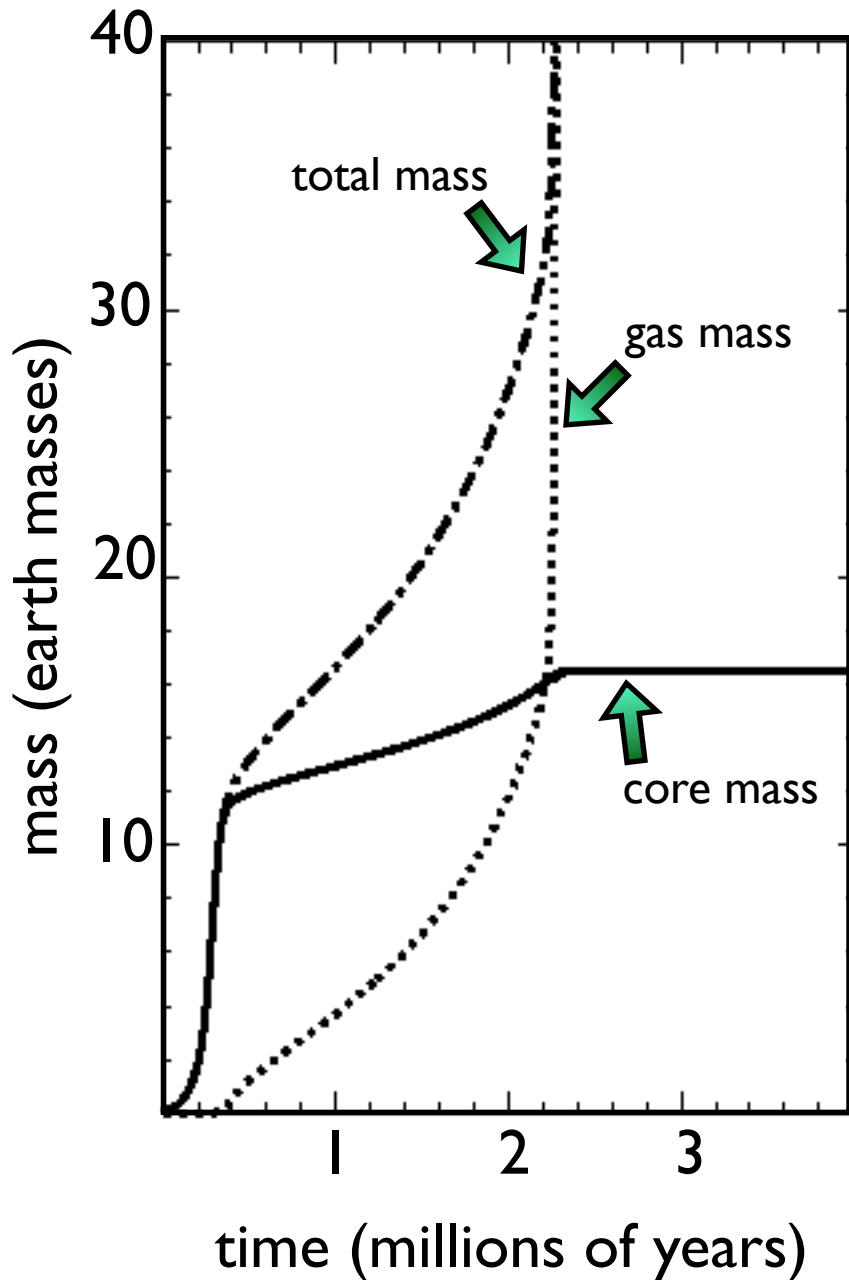


$\log \kappa$

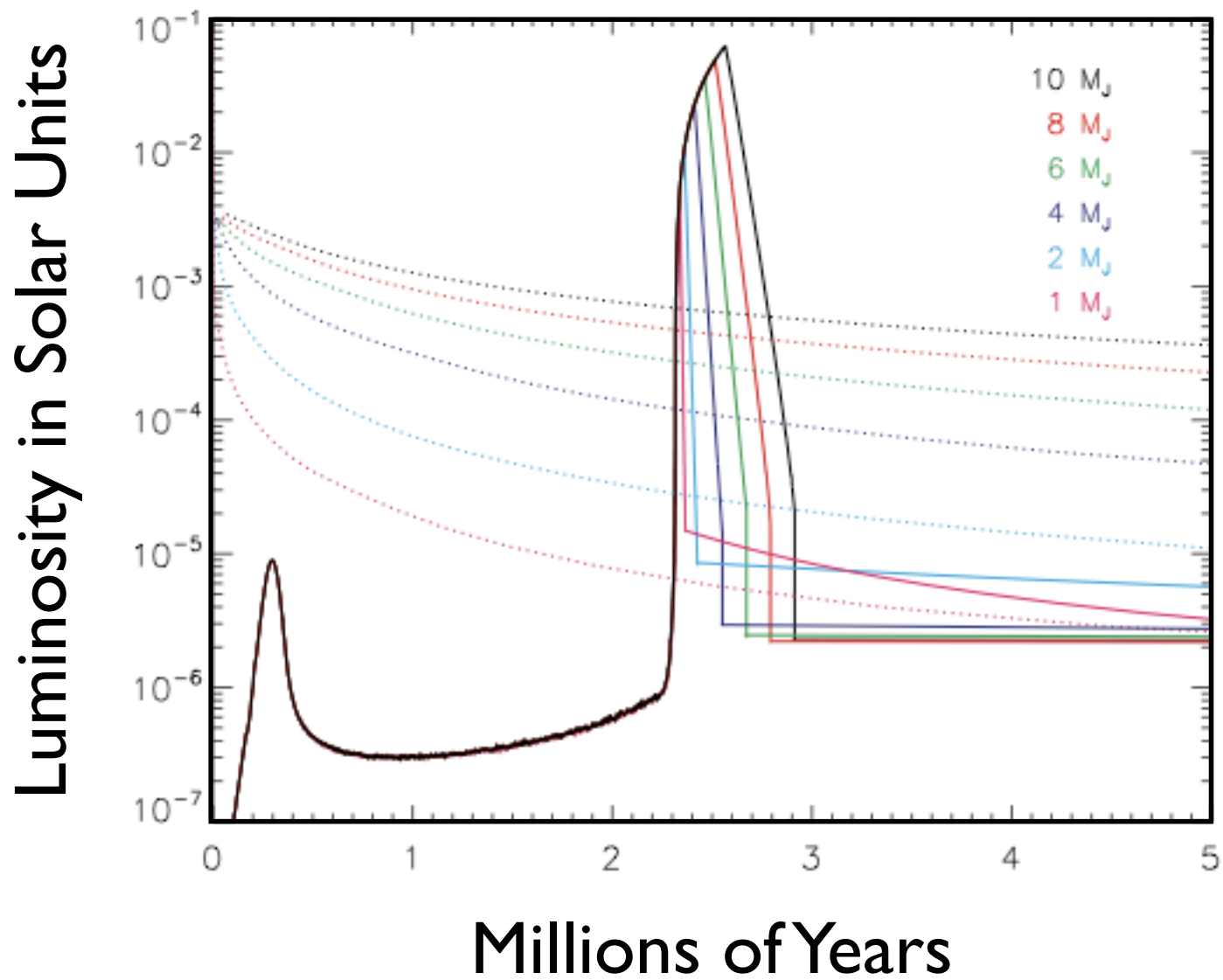


- Grain opacities are a key issue. Original studies (e.g Pollack et al 1996) used envelope opacities with an interstellar size distribution.
- But material that enters a giant planet envelope has been modified from the original interstellar grains by coagulation and fragmentation.
- Calculations by Podolak (2003) indicate that once grains enter the protoplanetary envelope, they coagulate and settle out quickly into warmer regions where they are destroyed. Podolak argues that true opacities are $\sim 50x$ smaller than interstellar.

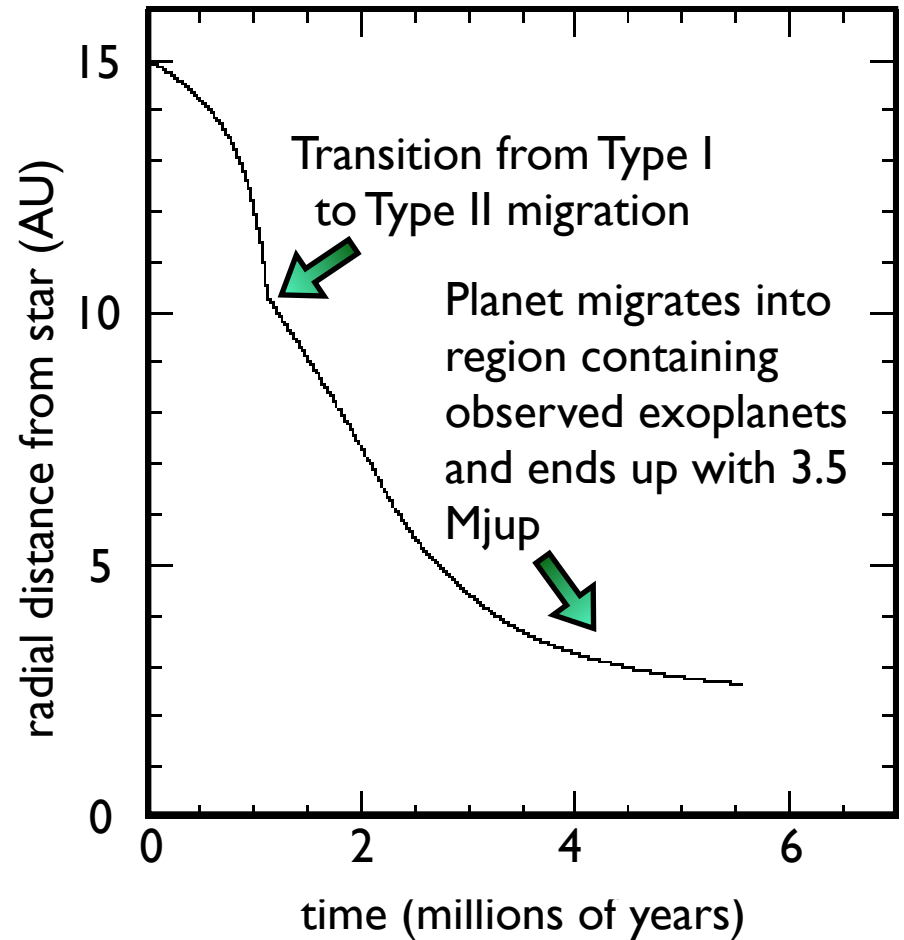
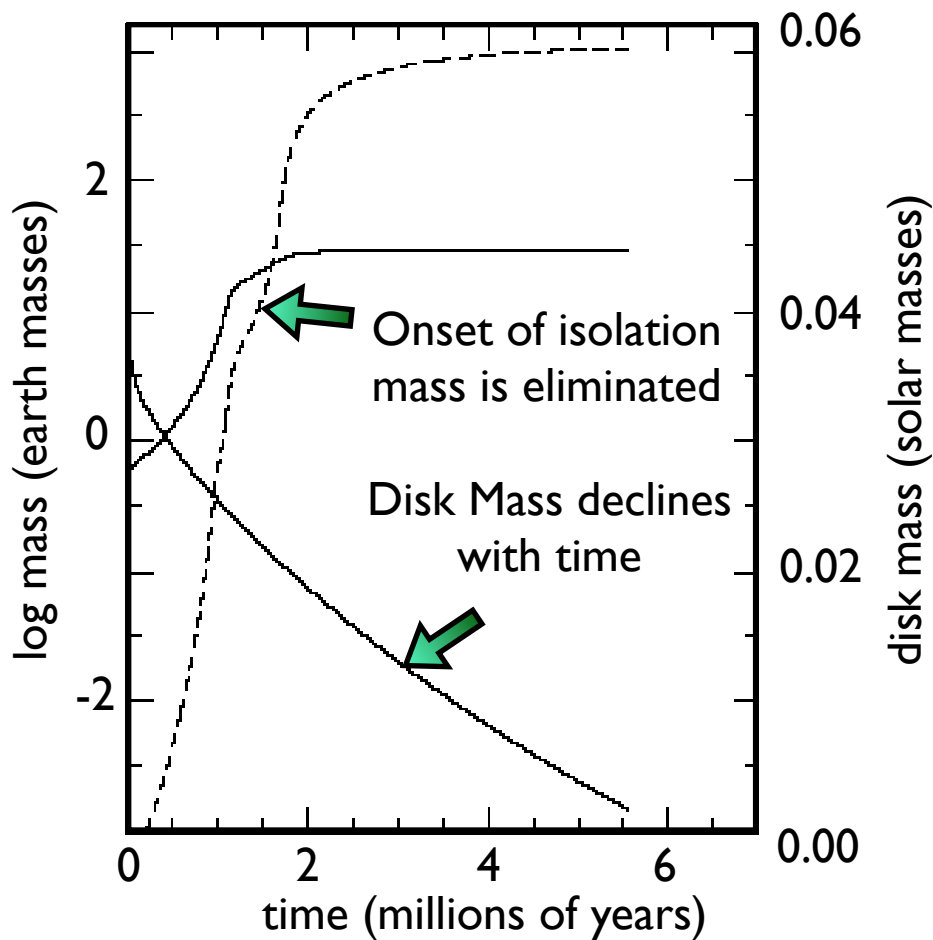
Reduced grain opacity greatly speeds up the gas accretion timescale.



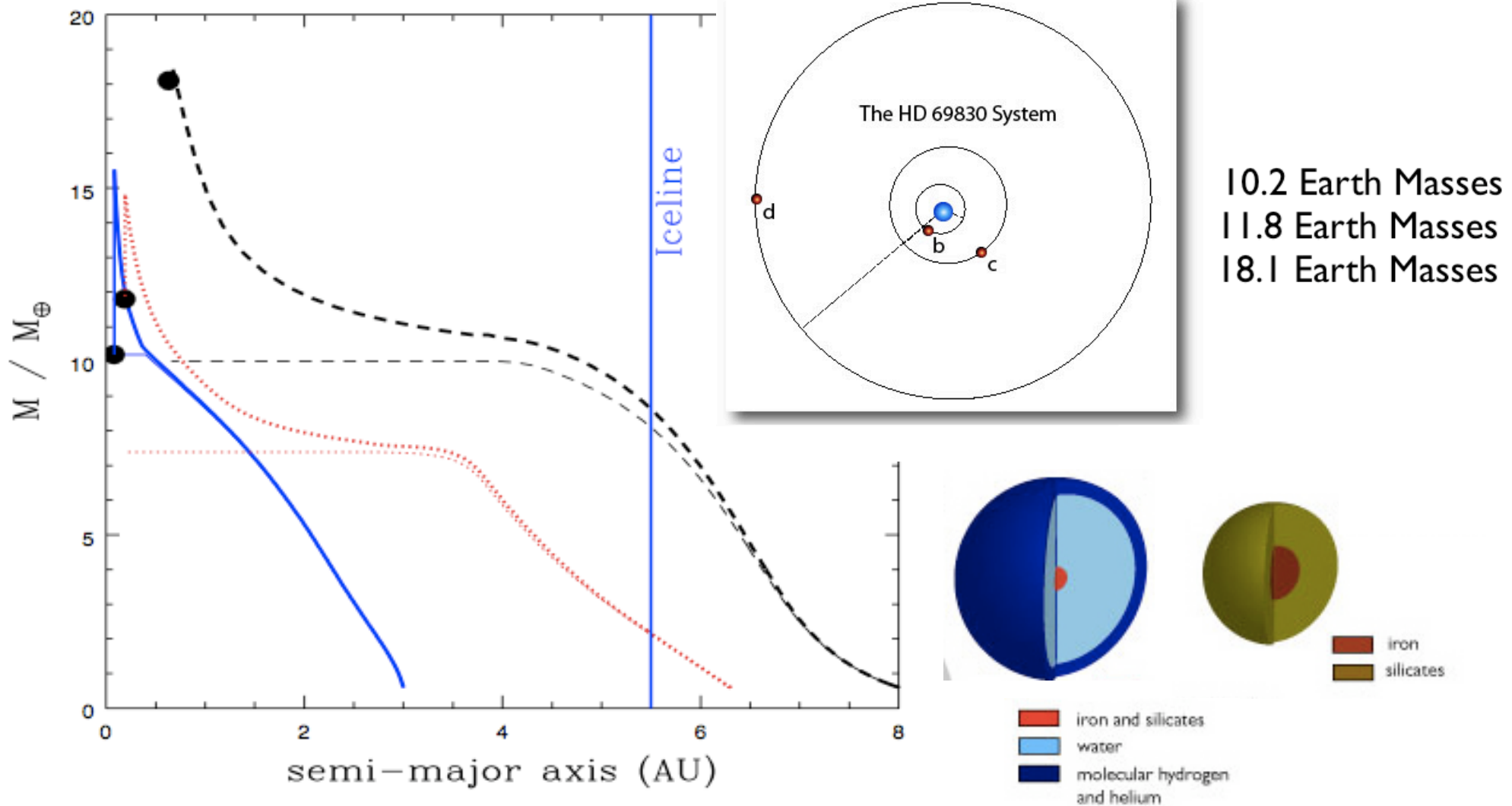
(Hubickyj et al. 2005)



Marley and collaborators (2007) have shown that core accretion leads to giant planets that are much fainter at early times than a high-entropy (“hot start”) initial condition would suggest. This has important consequences for direct imaging of exoplanets.

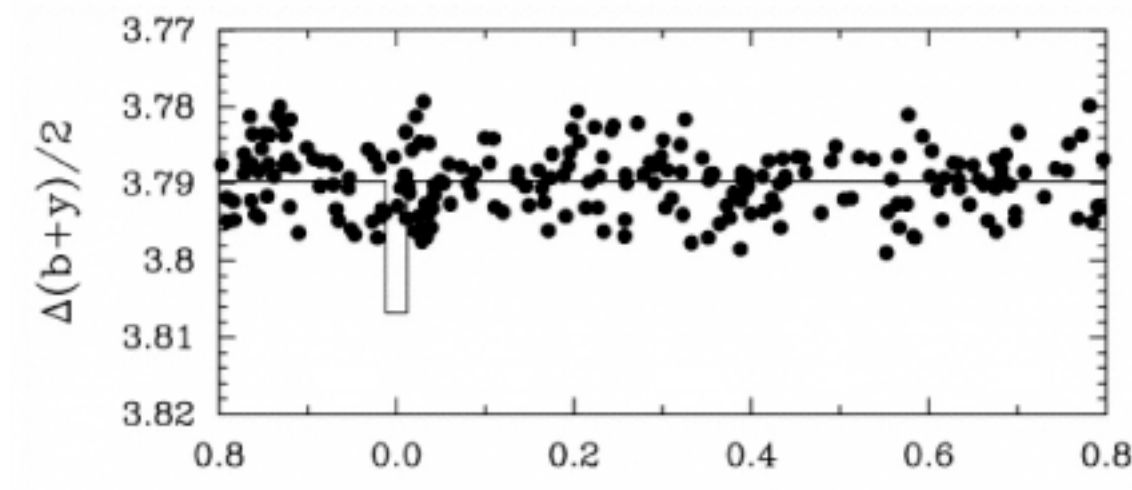


Alibert et al (2005, 2006) extended the core-accretion scenario to include migration, disk evolution, and gap formation. They find much reduced time-scales for the onset of rapid gas accretion.



Given after-the-fact modeling, the Alibert et al. framework can readily account for systems such as HD 69830 (which contains three neptune-mass planets). Models of this type make specific predictions for the composition, and hence the radii of the planets.

GI 436 was the first Neptune-mass planet discovered
(Butler et al. 2004)



Folded photometry (taken over a baseline of several years)
were interpreted as not indicating a transit.

Detection of transits of the nearby hot Neptune GJ 436 b

M. Gillon^{1,2}, F. Pont¹, B.-O. Demory^{1,3}, F. Mallmann³, M. Mayor¹, T. Mazeh⁴, D. Queloz¹, A. Shporer⁴,
S. Udry¹, C. Vuissoz⁵

¹ Observatoire de Genève, Université de Genève, 1290 Sauverny, Switzerland

² Institut d'Astrophysique et de Géophysique, Université de Liège, 4000 Liège, Belgium

³ Observatoire François-Xavier Bagnoud - OFXB, 3961 Saint-Luc, Switzerland

⁴ School of Physics and Astronomy, Raymond and Beverly Sackler Faculty of Exact Sciences, Tel Aviv University, Tel Aviv, Israel

⁵ Laboratoire d'Astrophysique, Ecole Polytechnique Fédérale de Lausanne (EPFL), Observatoire, 1290 Sauverny, Switzerland

Received date / accepted date

Abstract. This Letter reports on the photometric detection of transits of the Neptune-mass planet orbiting the nearby M-dwarf star GJ 436. It is by far the closest, smallest and least massive transiting planet detected so far. Its mass is slightly larger than Neptune's at $M = 22.6 \pm 1.9 M_{\oplus}$. The shape and depth of the transit lightcurves show that it is crossing the host star disc near its limb (impact parameter 0.84 ± 0.03) and that the planet size is comparable to that of Uranus and Neptune, $R = 25200 \pm 2200 \text{ km} = 3.95 \pm 0.35 R_{\oplus}$. Its main constituent is therefore very likely to be water ice. If the current planet structure models are correct, an outer layer of H/He constituting up to ten percent in mass is probably needed on top of the ice to account for the observed radius.

Key words. planetary systems – stars: individual: GJ 436 – techniques: photometry



OBSERVATOIRE

FRANÇOIS-XAVIER BAGNOUD

ST-LUC

[Home page](#)

[What's new ?](#)

Welcome to the new OFXB website !

Location & Organisation

The François-Xavier Bagnoud Observatory (OFXB) is located above Saint-Luc, a small village laying in Val d'Anniviers - swiss Alps, nearby Sierre. OFXB is managed by a non-profit-making foundation. This project became reality in 1995 thanks to the generosity of the [FXB foundation](#).

What OFXB offers...

The site where OFXB has been built benefits from the Alps legendary tranquility and beauty. Several summits above 4000m are easily visible, especially the Matterhorn, providing scenic landscapes. Furthermore, it is famous for pure and steady nights, especially suited for astronomy observing. From experimented amateur astronomers to schoolchildren, the Observatory welcomes all and features a full range of activities thanks to available facilities : 60cm reflector equipped with an high performance CCD camera, 15cm apochromatic refractor and a fully equipped auditorium for 3D shows and conferences. Kitchen and lavatories are available for visitors. A funicular links the Observatory from the village.

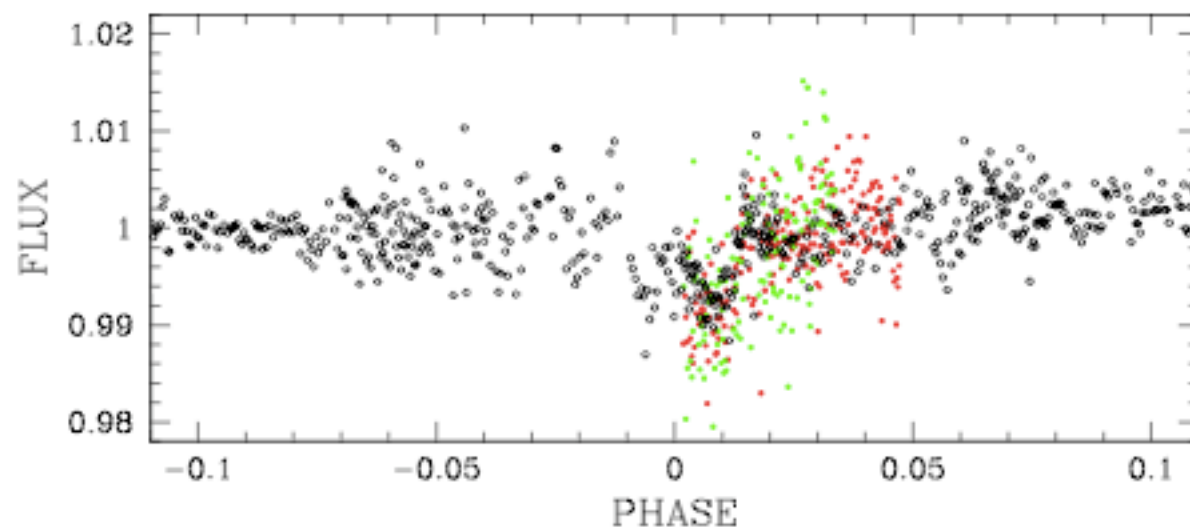


Fig. 1. OFXB (*black*) and Wise (*red: 1m, green: 46cm*) photometry phase-folded using the ephemerids and period presented in Maness et al. (2007).

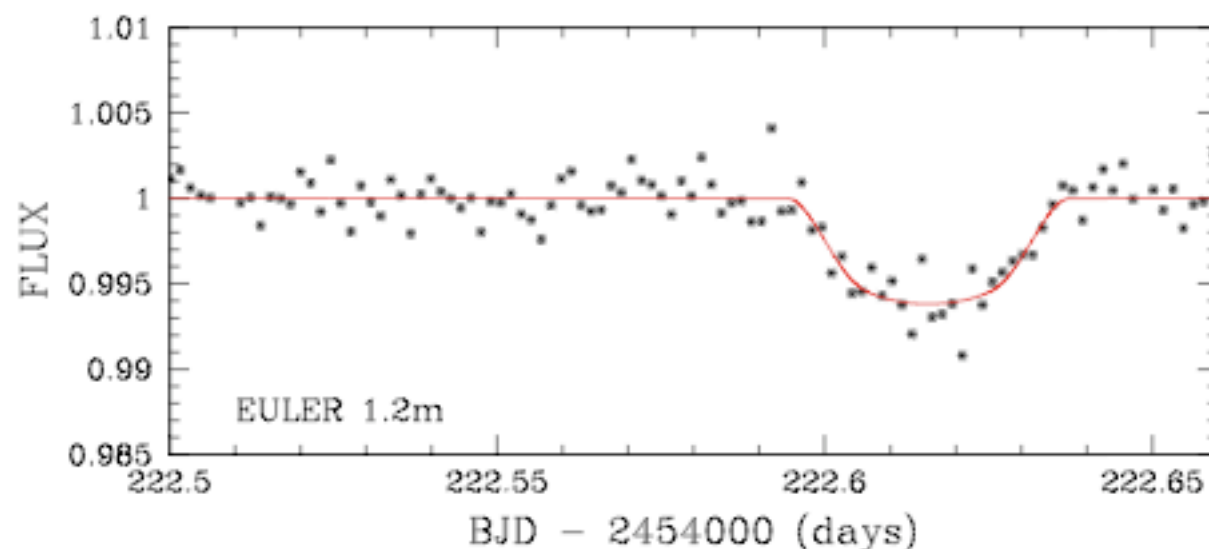
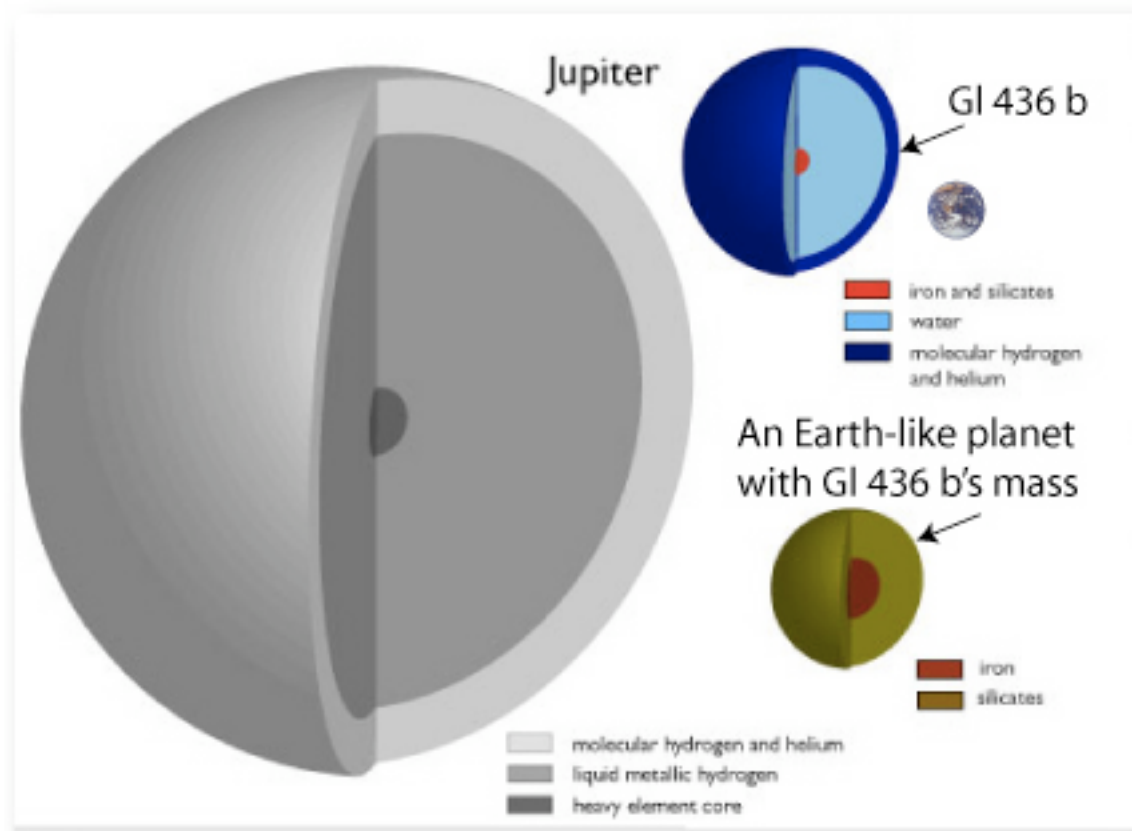
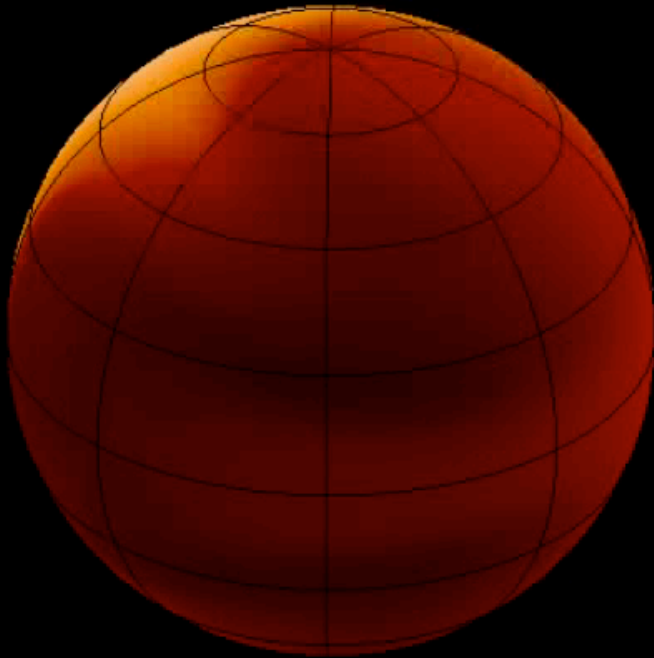


Fig. 2. Euler V-band transit photometry. The best-fit transit curve is superimposed in red.

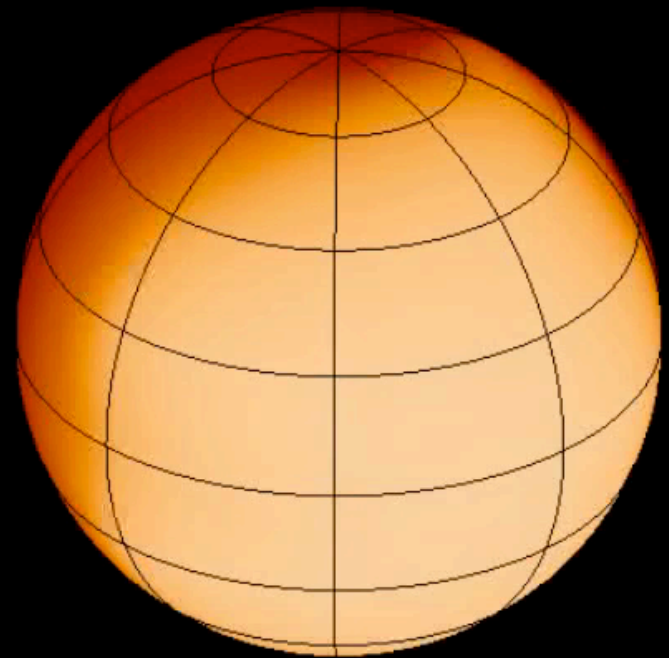


Gl 436 is made mostly of water. It migrated to its current location

Weather forecast for Gl 436b (2 full orbits)

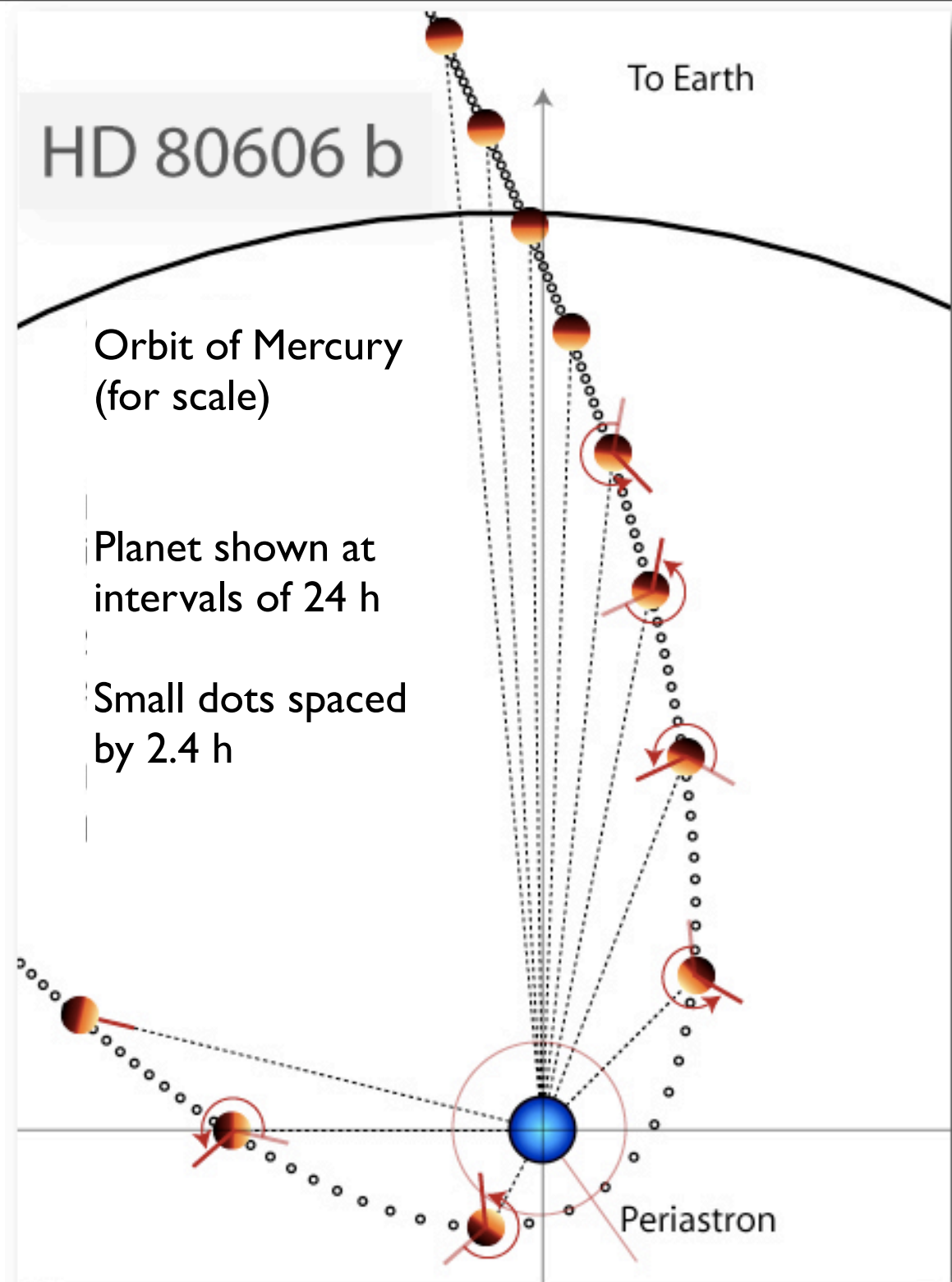
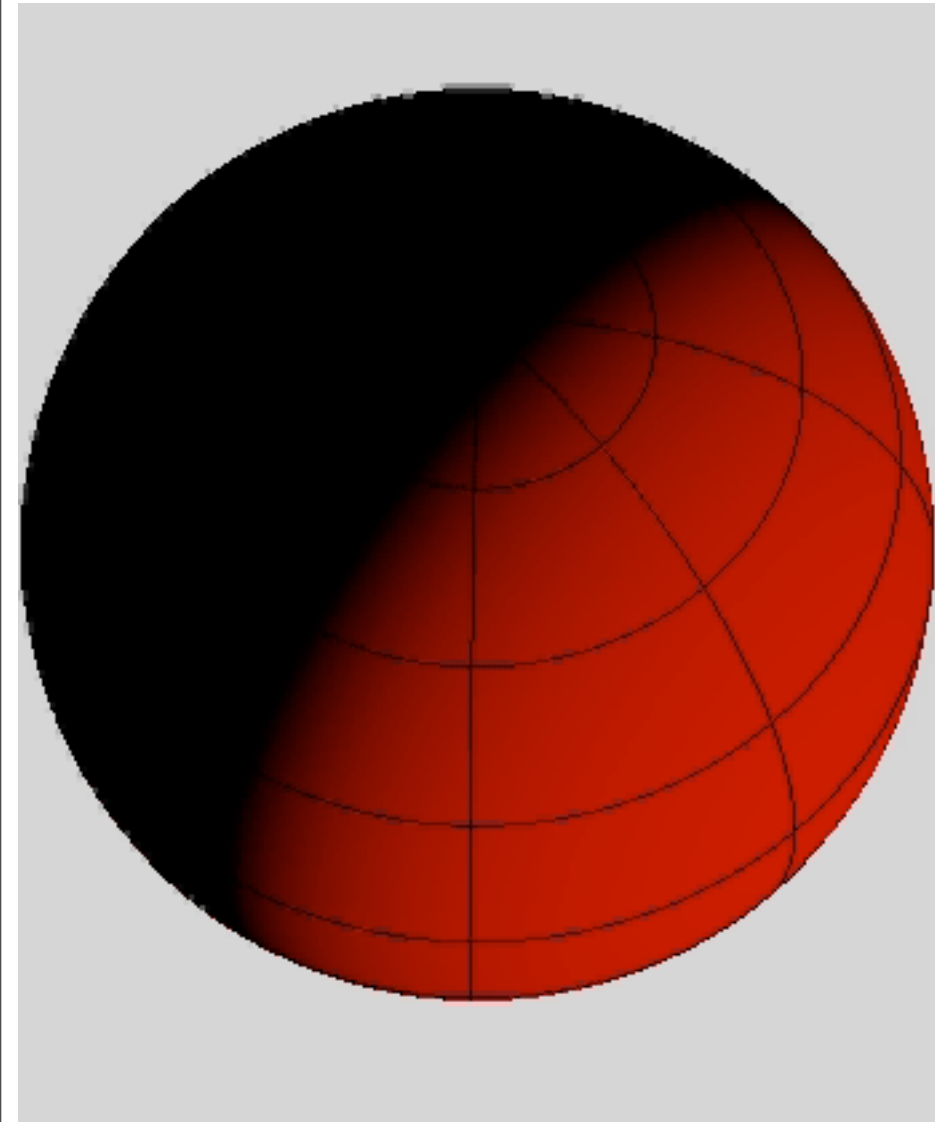


Western Hemisphere

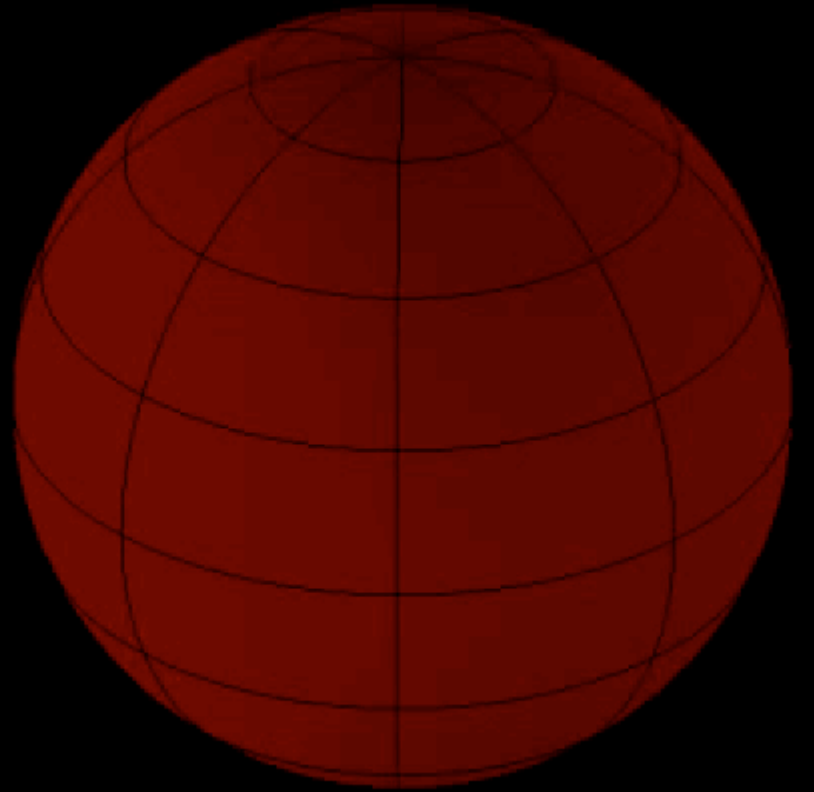
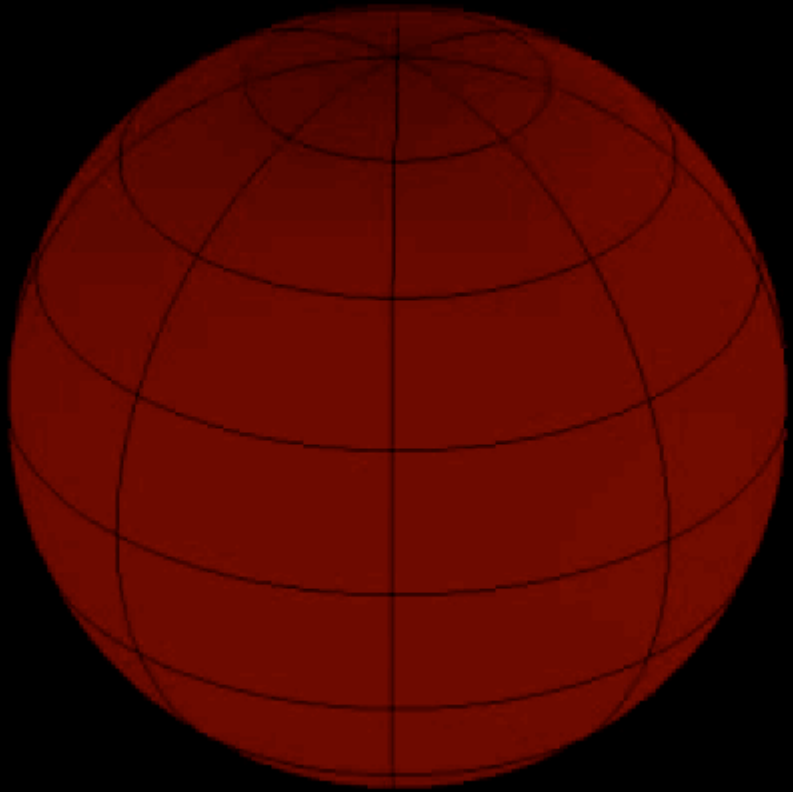


Eastern Hemisphere

Irradiation at Periastron

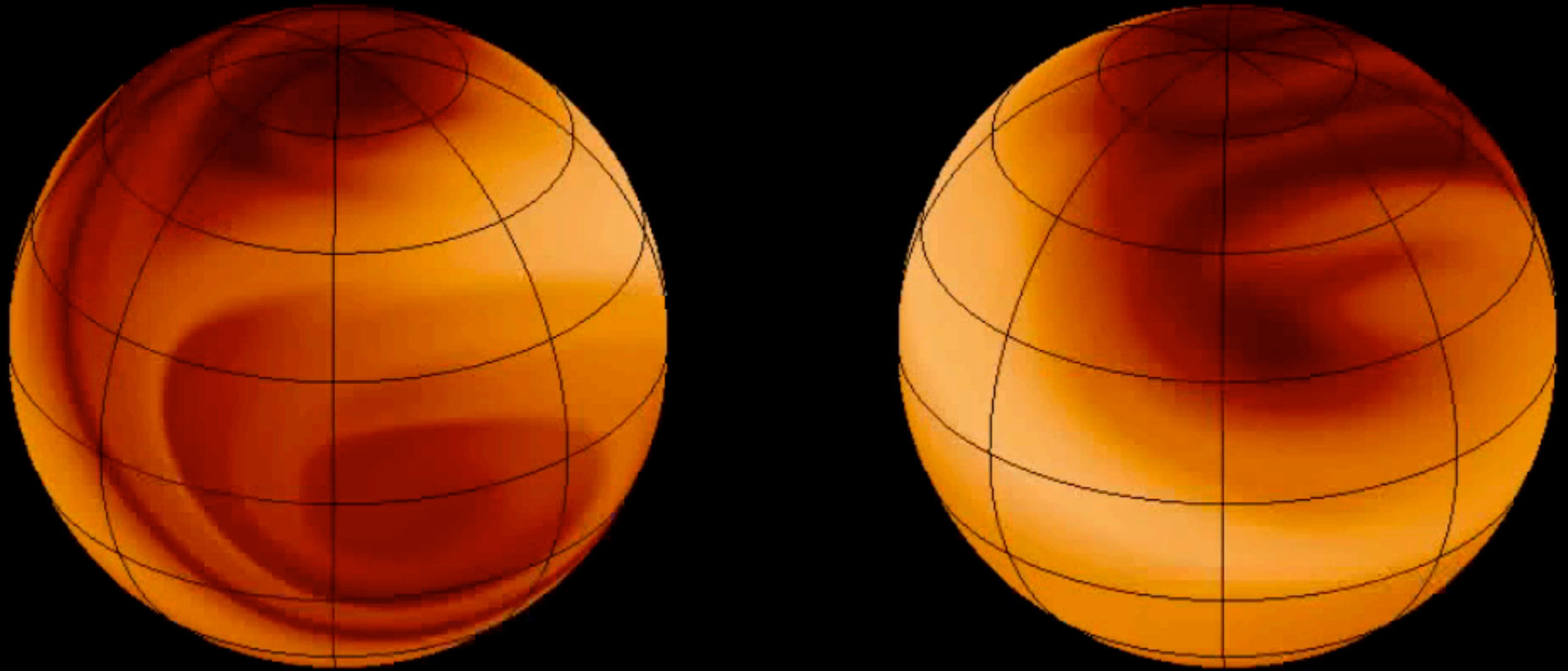


HD 80606 b



Temperature Range: 700 K to 1200K

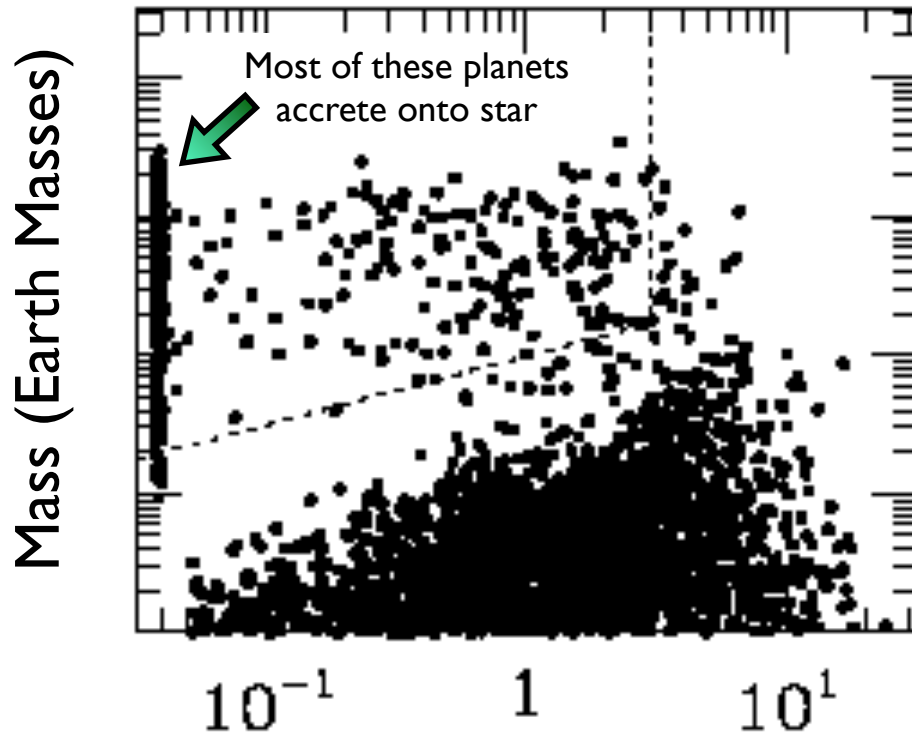
HD 185269 b



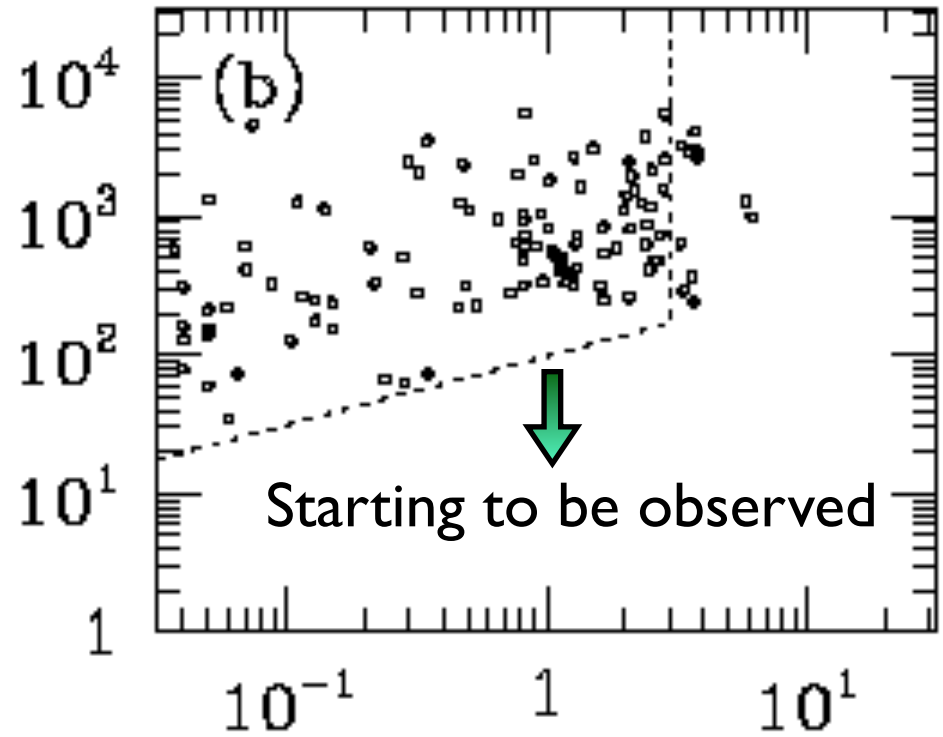
Temperature Range: 900K to 1760K

Ida & Lin Model Distribution

Observed Distribution



Semi-Major Axis (AU)

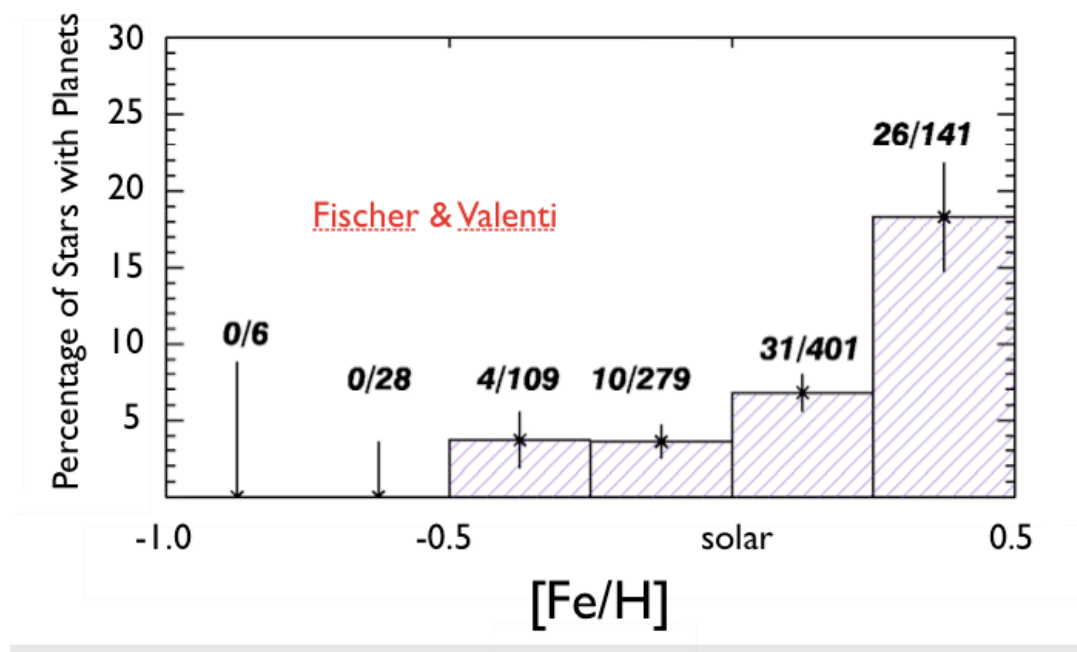


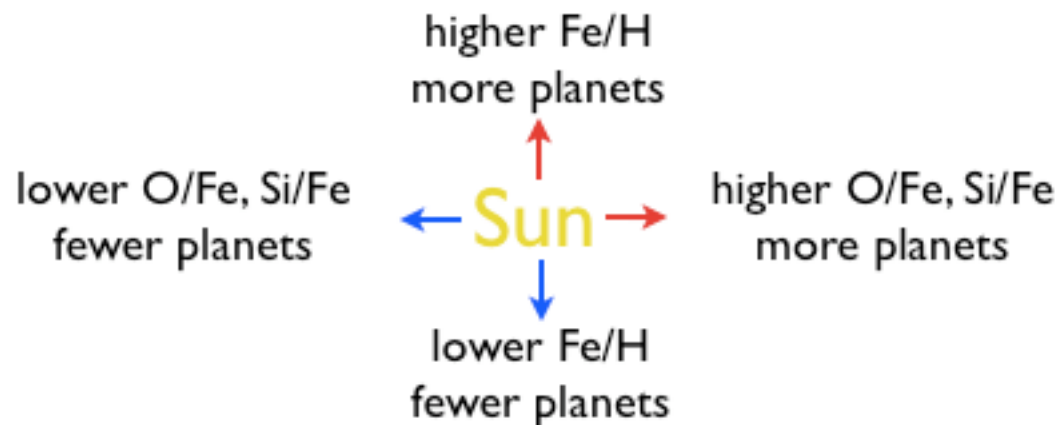
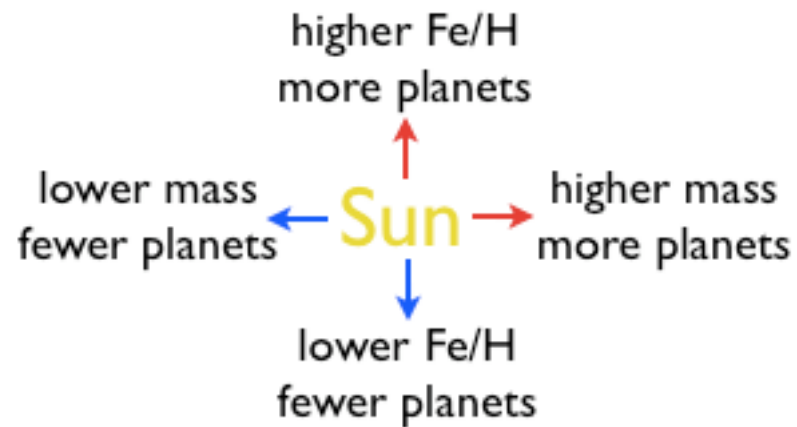
Semi-Major Axis (AU)

Ida and Lin (2004, 2005, 2006), Korneet et al. (2005), and Robinson et al. (2006) carried out a large number of Monte-Carlo simulations which draw from distributions of disk masses and seed-planetesimals to model the process of core accretion. These simulations always reproduce the planet “desert”, and predict a huge population of terrestrial and ice giant planets somewhat below the current detection threshold for radial velocity surveys.

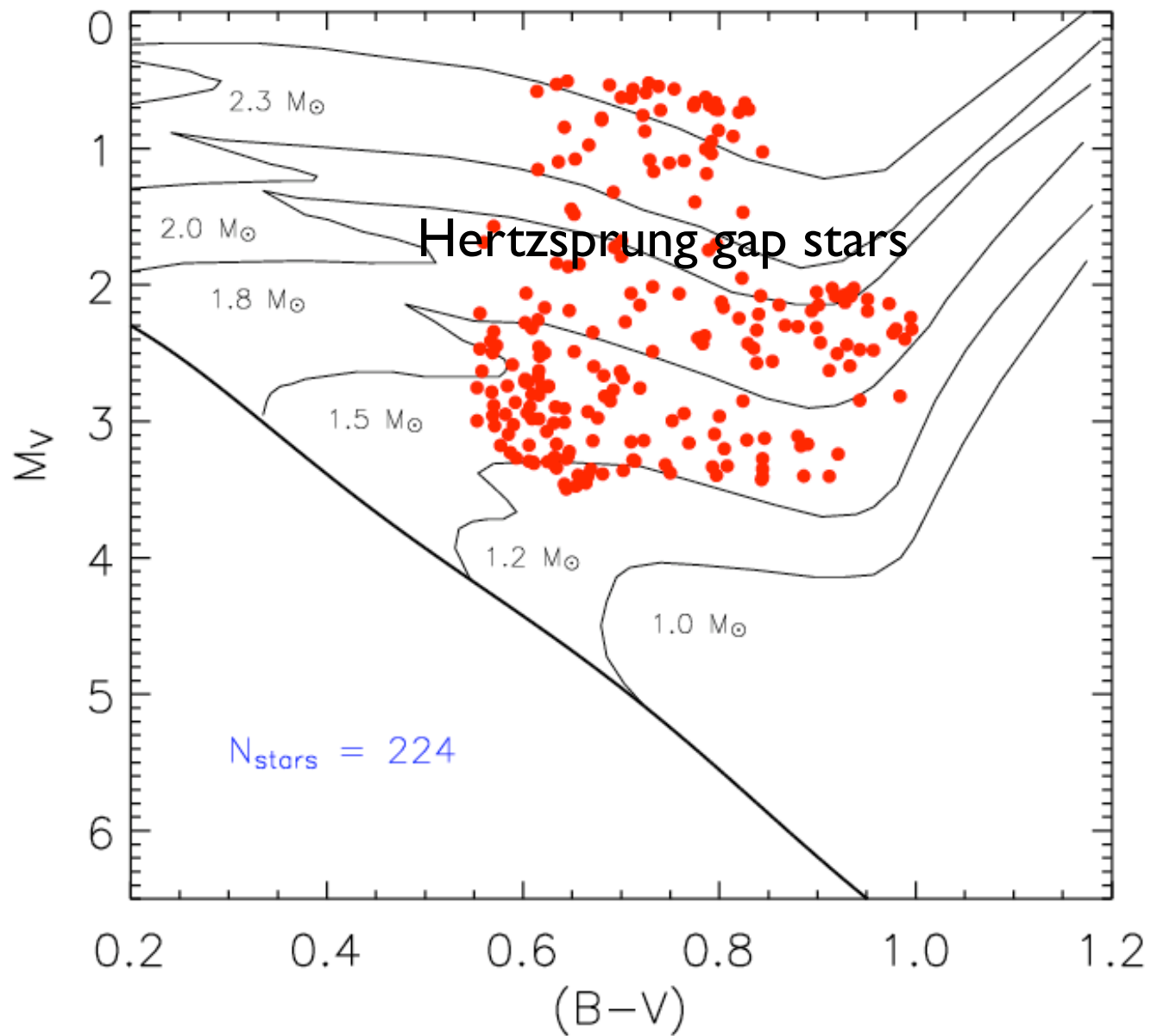
A key (and well-established) result of the core accretion theory is the extraordinary sensitivity of the time of onset of rapid gas accretion to the surface density of solids in the disk.

Calculations by Hubickyj et al (2005) find that decreasing the solid surface density from 10 to 6 gm/cm² causes a 12 Myr delay in the onset of rapid gas accretion. This leads to a variety of observational opportunities to test the basic model. For example, this solid surface density decrease corresponds to a ~0.2 dex decrease in metallicity. It's likely a major factor underlying the observed planet-metallicity correlation:



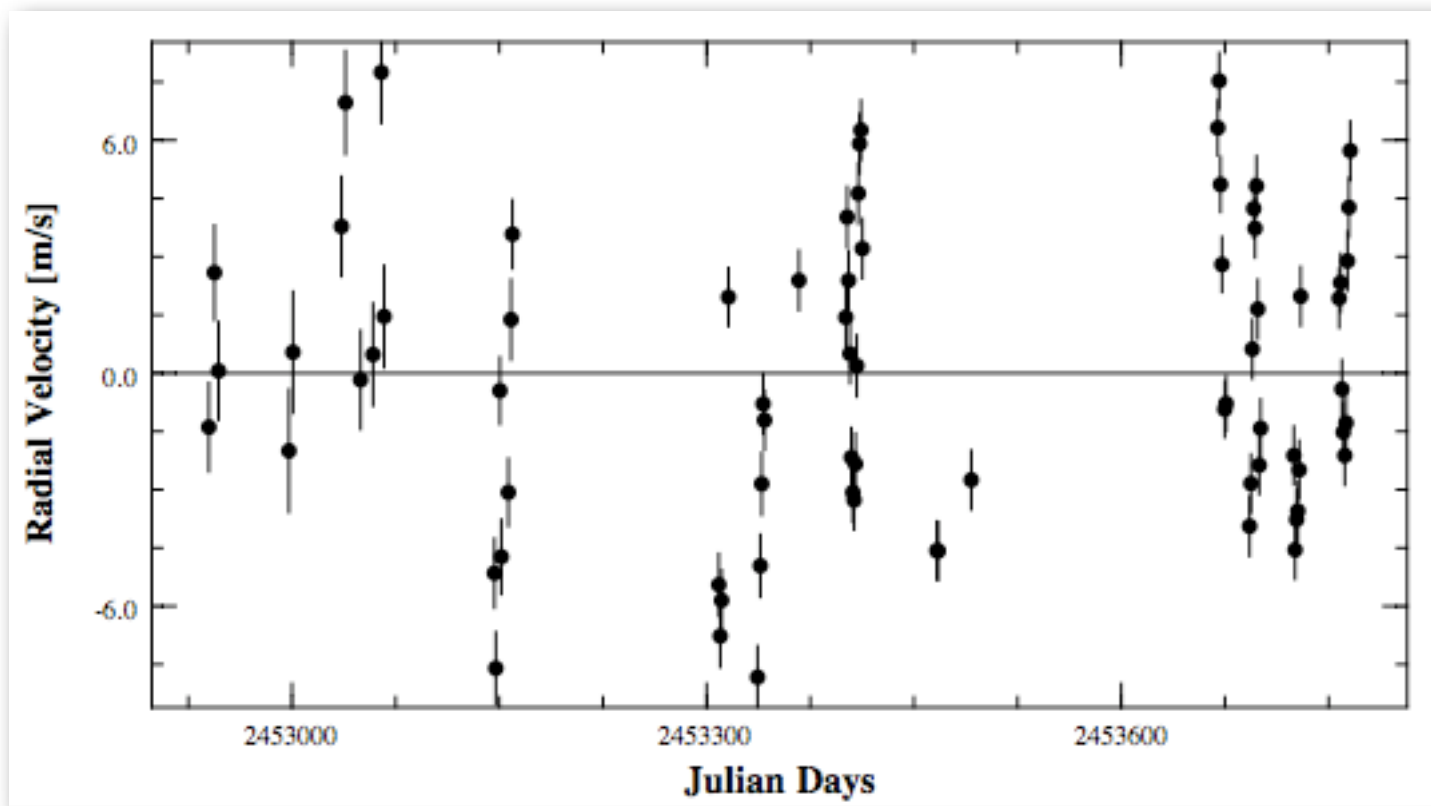


Trends that should exist for post-core accretion Jovian planets.



The relative planeticity of higher mass stars can be explored via both RV (John Johnson's thesis RV survey, and Bunei Sato's ongoing RV survey) and also by transit surveys (when they reach sufficient numbers of planets for statistical inferences).

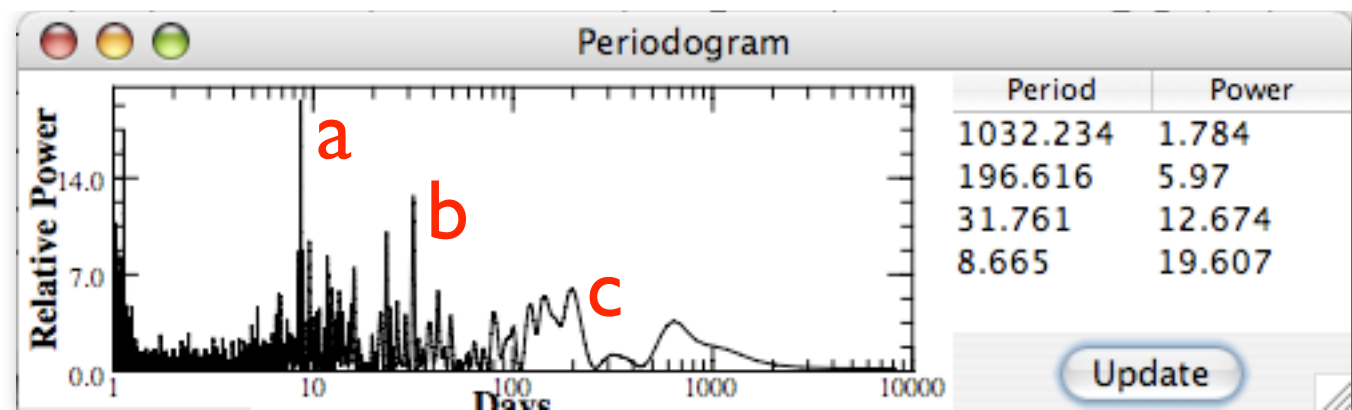
The HD 69830 Detection is a Groundbreaking Discovery



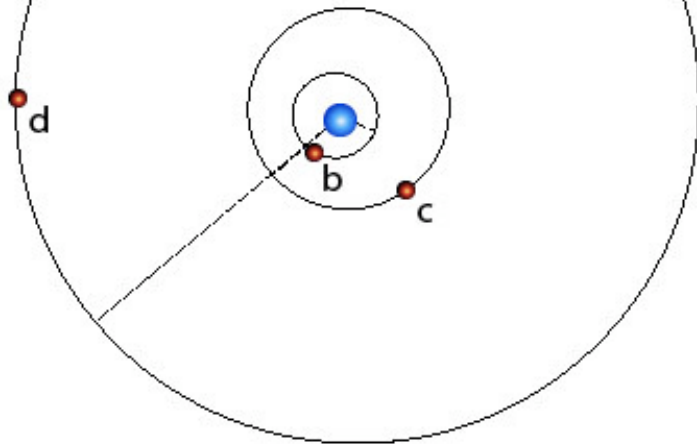
6 m/s

0.86 Msun

< 1 m/s “jitter”



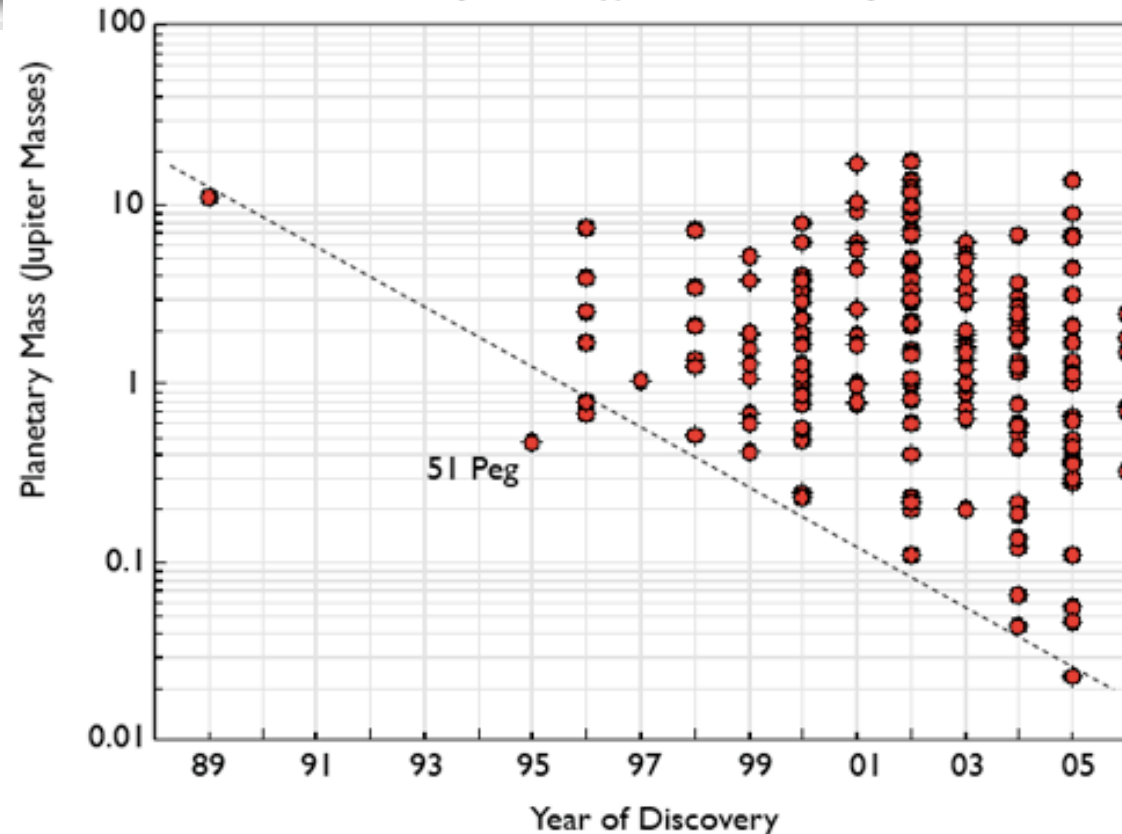
The HD 69830 System

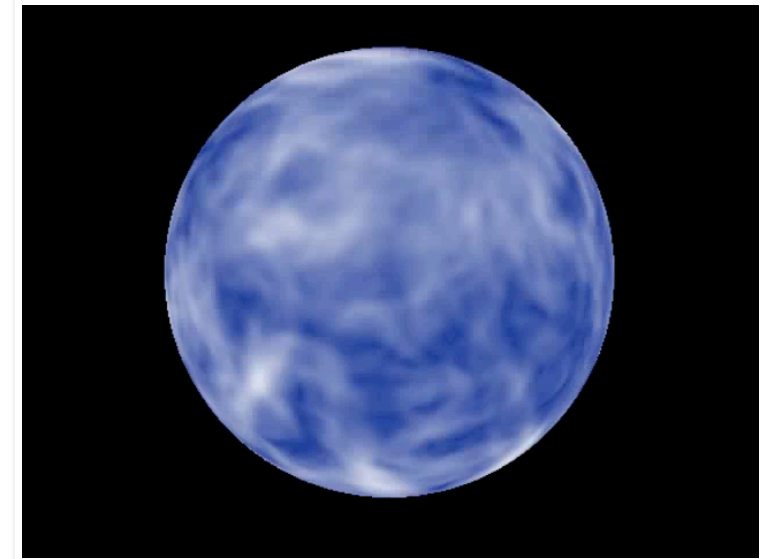
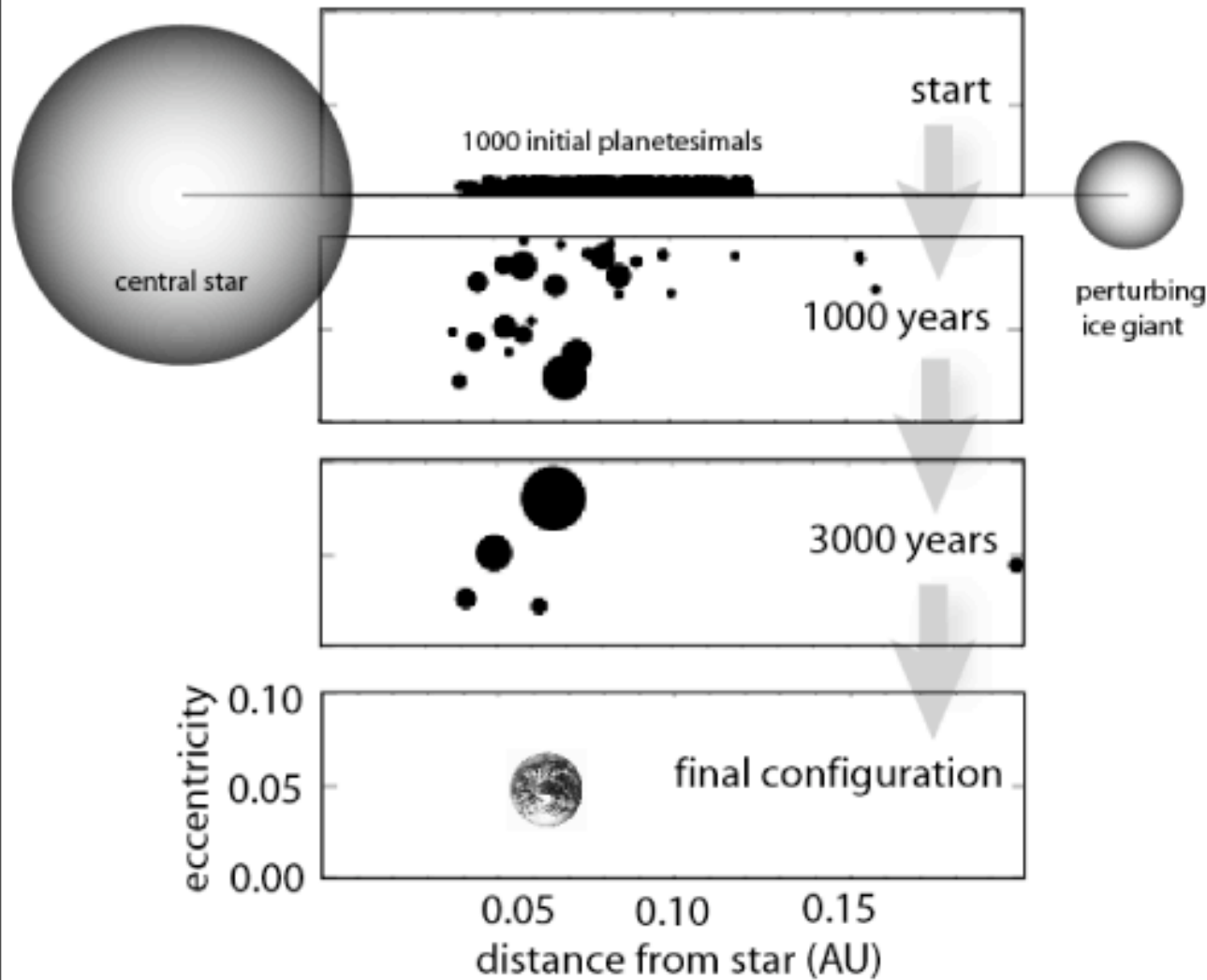


10.2 Earth Masses
11.8 Earth Masses
18.1 Earth Masses

The error on the half-amplitude, K , for planet b is 0.2 m/s

Planetary $M \sin(i)$ vs. Discovery Year





Hydrodynamical simulation of the atmospheric flow on Gl 581c

Our simulations of planet formation are indicating that it's very likely that Earth-size planets are common on short-period orbits around low-mass stars.

I predict that within a year, there will be an RV+photometric ground-based detection of a potentially habitable planet transiting an M dwarf.